THE UNIVERSITY of EDINBURGH

Edinburgh Research Explorer

Feedback loop promotes sucrose accumulation in cotyledons to facilitate sugar ethylene signaling mediated, etiolated seedling greening

Citation for published version:
Mu, XR, Tong, C, Fang, XT, Bao, Q-X, Xue, LN, Meng, W-Y, Liu, CY, Loake, GJ, Cao, XY, Jiang, J-H & Meng, L-S 2022, 'Feedback loop promotes sucrose accumulation in cotyledons to facilitate sugar ethylene signaling mediated, etiolated seedling greening', *Cell Reports*, vol. 38, no. 11, 110529. https://doi.org/10.1016/j.celrep.2022.110529

Digital Object Identifier (DOI):
10.1016/j.celrep.2022.110529

Link:
Link to publication record in Edinburgh Research Explorer

Document Version:
Publisher's PDF, also known as Version of record

Published In:
Cell Reports

General rights
Copyright for the publications made accessible via the Edinburgh Research Explorer is retained by the author(s) and / or other copyright owners and it is a condition of accessing these publications that users recognise and abide by the legal requirements associated with these rights.

Take down policy
The University of Edinburgh has made every reasonable effort to ensure that Edinburgh Research Explorer content complies with UK legislation. If you believe that the public display of this file breaches copyright please contact openaccess@ed.ac.uk providing details, and we will remove access to the work immediately and investigate your claim.

OPEN ACCESS

Download date: 17. May. 2022

Cell Reports

Article

Feedback loop promotes sucrose accumulation in cotyledons to facilitate sugar-ethylene signaling-mediated, etiolated-seedling greening

Graphical abstract

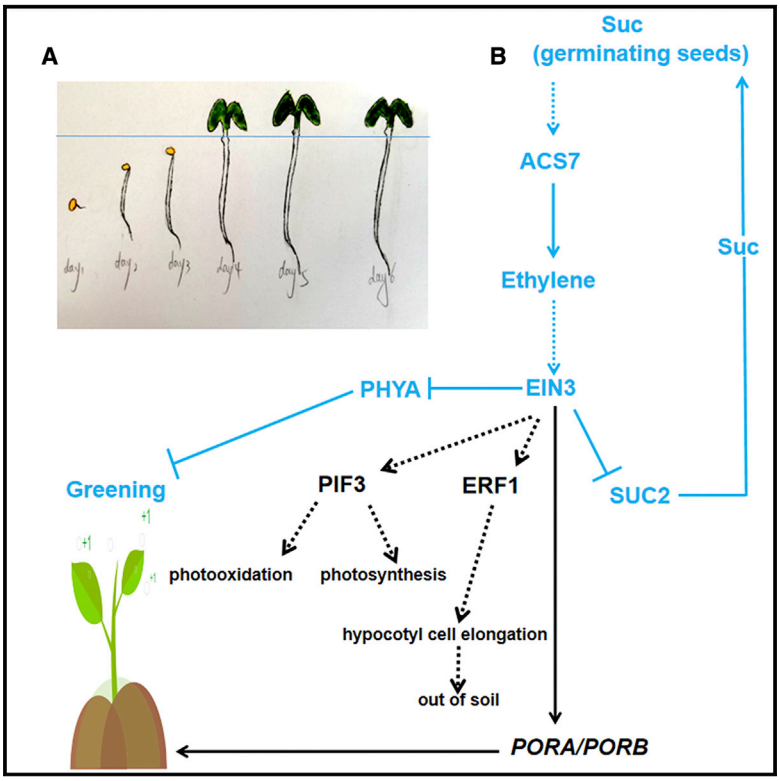

Highlights

- Sucrose feedback signaling promotes its accumulation in cotyledons under darkness
- Accumulated sucrose in cotyledons stimulates ethylene biosynthesis to enable greening

Authors

Xin-Rong Mu, Chen Tong, Xing-Tang Fang, ..., Xiao-Ying Cao, Ji-Hong Jiang, Lai-Sheng Meng

Correspondence

menglsh@jsnu.edu.cn (L.-S.M.), jhjiang@jsnu.edu.cn (J.-H.J.), cxy4868@jsnu.edu.cn (X.-Y.C.)

In brief

Mu et al. describe a sucrose-signaling feedback loop (Suc-ACS7-EIN3-|SUC2-Suc) that promotes sucrose accumulation of cotyledons under darkness. This promotes ethylene biosynthesis, facilitates de-etiolation, and enables seedlings to green and grow out of soil when seedlings are exposed to light from darkness.

Mu et al., 2022, Cell Reports *38*, 110529
March 15, 2022 © 2022 The Authors.
https://doi.org/10.1016/j.celrep.2022.110529

CellPress

Cell Reports

CellPress
OPEN ACCESS

Article

Feedback loop promotes sucrose accumulation in cotyledons to facilitate sugar-ethylene signaling-mediated, etiolated-seedling greening

Xin-Rong Mu,[1] Chen Tong,[1] Xing-Tang Fang,[2] Qin-Xin Bao,[1] Li-Na Xue,[1] Wei-Ying Meng,[1] Chang-Yue Liu,[1] Gary J. Loake,[3,4,] Xiao-Ying Cao,[1,*] Ji-Hong Jiang,[1,*] and Lai-Sheng Meng[1,5,*]

[1]The Key Laboratory of Biotechnology for Medicinal Plants of Jiangsu Province, Jiangsu Normal University, Xuzhou, Jiangsu 221116, People's Republic of China

[2]School of Life Science, Jiangsu Normal University, Xuzhou, Jiangsu 221116, People's Republic of China

[3]Jiangsu Normal University, Edinburgh University, Centre for Transformative Biotechnology of Medicinal and Food Plants, Jiangsu Normal University, 101 Shanghai Road, Xuzhou, Jiangsu 221116, People's Republic of China

[4]Institute of Molecular Plant Sciences, School of Biological Sciences, Edinburgh University, King's Buildings, Mayfield Road, Edinburgh EH9 3JR, UK

[5]Lead contact

*Correspondence: menglsh@jsnu.edu.cn (L.-S.M.), jhjiang@jsnu.edu.cn (J.-H.J.), cxy4868@jsnu.edu.cn (X.-Y.C.)

https://doi.org/10.1016/j.celrep.2022.110529

SUMMARY

De-etiolation is indispensable for seedling survival and development. However, how sugars regulate de-etiolation and how sugars induce ethylene (ET) for seedlings to grow out of soil remain elusive. Here, we reveal how a sucrose (Suc) feedback loop promotes de-etiolation by inducing ET biosynthesis. Under darkness, Suc in germinating seeds preferentially induces *1-amino-cyclopropane-1-carboxylate synthase* (*ACS7*; encoding a key ET biosynthesis enzyme) and associated ET biosynthesis, thereby activating ET core component ETHYLENE-INSENSITIVE3 (EIN3). Activated EIN3 directly inhibits the function of Suc transporter 2 (SUC2; a major Suc transporter) to block Suc export from cotyledons and thereby elevate Suc accumulation of cotyledons to induce ET. Under light, ET-activated EIN3 directly inhibits the function of phytochrome A (phyA; a de-etiolation inhibitor) to promote de-etiolation. We therefore propose that under darkness, the Suc feedback loop (Suc-ACS7-EIN3-|SUC2-Suc) promotes Suc accumulation in cotyledons to guarantee ET biosynthesis, facilitate de-etiolation, and enable seedlings to grow out of soil.

INTRODUCTION

The light-dependent switch from skotomorphogenesis to photomorphogenesis is essential for seedling survival. In the life cycle of a plant, the first step is seedling establishment after seed germination under darkness. During this process, seedlings develop elongated hypocotyls and suppressed cotyledons. These dark-grown seedlings are capable of utilizing sucrose (Suc) as their main energy source. Suc is mainly derived from oil bodystored neutral lipids, triacyclglycerols (TAGs), which are considered a main energy source for postgerminative growth (Mazzella et al., 2014). Glyoxysomes are present in cotyledons of etiolated seedlings, and they are specialized peroxisomes engaged in the degradation of TAGs by both the glyoxylate cycle and β-oxidation (Graham, 2008). In *Arabidopsis*, the loss of glyoxylate-cycle enzymes (glyoxysome mutants), for example, isocitrate lyase (ICL) and malate synthase (MLS), shows a distinctive characteristic of sugar starvation after germination due inability to convert stored lipids into Suc (Eastmond et al., 2000; Cornah et al., 2004).

The second step is that germinating seedlings undergo photomorphogenesis upon light irradiation, including hypocotyl shortening, and cotyledon opening and greening (i.e., chlorophyll biosynthesis), allowing seedlings to turn photosynthetically autotrophic and competent (Zhong et al., 2009, 2014). Specifically, during this process, seedlings exhibit a decreased hypocotyl growth rate, the cotyledons begin to unfold, the apical hook starts to open, and, significantly, the initiation of cholorophyll biosynthesis drives cotyledon greening. Therefore, white light is the major factor triggering the cotyledon-greening process of etiolated seedlings (Mazzella et al., 2014).

The E3 ubiquitin ligase constitutively photomorphogenic 1 (COP1) is a key suppressor of photomorphogenesis and has been reported to be indispensable in regulating cotyledon greening (Moon et al., 2008; Zhong et al., 2009). In addition, phytochrome-interacting factors (PIFs) are also thought to play a fundamental role in regulating the switch from skoto- to photomorphogenesis (Zhong et al., 2009; Duek and Fankhauser, 2005). For example, PIF1 and PIF3 facilitate cotyledon greening partly via suppressing protochlorophyllide accumulation under darkness (Duek and Fankhauser, 2005; Stephenson et al., 2009).

Ethylene (ET), a gaseous hormone, is also thought to be integral to the regulation of cotyledon greening. In this context, ET

This is an open access article under the CC BY-NC-ND license (http://creativecommons.org/licenses/by-nc-nd/4.0/).

and PIF1 redundantly regulate the skoto-to-photomorphogenesis transition by facilitating cotyledon greening upon light irradiation (Zhong et al., 2009). Activation of a key ET signaling component, ETHYLENE-INSENSITIVE3 (EIN3), a plant-specific transcription factor, with an N-terminal DNA-binding domain and a unique fold structure, is both necessary and sufficient for seedling greening (Zhong et al., 2009). Under darkness, ET facilitates the greening of etiolated seedlings by EIN3 directly binding to the promoters of protochlorophyllide oxidoreductase A/B (*PORA/B*) (Zhong et al., 2009). Further, the mechanical stress of the soil activates ET production to promote cotyledon greening by a key ET component, EIN3, activating a PIF3-ERF1 (ET response factor 1) transcriptional circuitry to synchronize tissue-specific developments (Zhong et al., 2014). However, whereas the mechanical stress of the soil activates ET production and, in turn, promotes cotyledon greening by EIN3 controlling a few phytochrome and associated factors, how the mechanical stress of the soil induces ET production remains unclear.

Whereas white light is the major factor triggering the cotyledon-greening process of etiolated seedlings, far-red light inhibits this phenomenon by decreasing the level of PORA/B, which catalyzes the light-dependent reduction of protochlorophyllide A to chlorophyllide A, which is subsequently converted to chlorophyll (Barnes et al., 1996; Sperling et al., 1997). Interestingly, continuous far-red irradiation suppresses cotyledon greening in *Arabidopsis*, which can be restored by exogenously applied Suc (Barnes et al., 1996), suggesting that sugars may promote etiolated-seedling greening.

Sugars affect many aspects of growth and development throughout the plant life cycle, including germination, flowering, and senescence. Suc is a major soluble sugar in seed embryos and is also the predominant transported sugar in *Arabidopsis*, with phloem loading essential for plant growth, development, and reproduction (Chen et al., 2012). In *Arabidopsis*, phloem-specific sucrose transporter 2 (SUC2) is specifically expressed in companion cells (Stadler and Sauer, 1996) and has a central role in the phloem loading of Suc, which is essential for high-performance Suc transport from source to sink tissues (Stadler and Sauer, 1996; Gottwald et al., 2000; Srivastava et al., 2008). *suc2* mutants exhibit stunted growth, delayed development, and sterility. Further, this line accumulates starch and Suc in leaf blades and is blocked in the transport of sugars to sink organs, including the shoot apex, inflorescences, and roots (Gottwald et al., 2000).

Suc is a major soluble sugar in seed embryos and is also the predominant transported sugar in *Arabidopsis*, and continuous far-red irradiation suppresses cotyledon greening in *Arabidopsis*, which can be restored by the exogenous application of Suc (Barnes et al., 1996). This suggests that Suc may promote etiolated-seedling greening. Therefore, it should be investigated if Suc promotes cotyledon greening by regulating the phloem loading of Suc.

Here, we identify a Suc feedback loop and demonstrate that, under darkness, this Suc feedback loop following seed germination promotes Suc accumulation in cotyledons. When cotyledons are exposed to light from darkness, accumulated Suc in cotyledons stimulates ET biosynthesis to promote sugar-ET signaling-mediated, etiolated-seedling greening. Specifically, under darkness, *ACS7* expression and associated ET biosynthesis are induced preferentially by accumulated Suc in germinating seeds. Induced ET enhances EIN3 activity, which in turn directly suppresses the function of the key Suc transporter SUC2, thereby inhibiting Suc phloem loading in cotyledons. Consequently, the exporting Suc from cotyledons is inhibited. Therefore, Suc accumulation is enhanced by the Suc feedback loop. On seedling emergence and concomitant exposure to white light irradiation, accumulated Suc stimulates ET biosynthesis. ET-activated EIN3 negatively regulates phytochrome A (phyA), an inhibitor of etiolated-seedling greening, promoting this key developmental process. Collectively, this enables the possibility of specifically manipulating both Suc accumulation and ET production and associated signaling in mesophyll cells to enable coordination of both Suc phloem loading and ET signaling in cotyledons with a few phytochrome and associated factors (including phyA) without disturbing the whole plant body plan.

RESULTS

The cotyledon greening of etiolated seedlings was promoted by endogenous sugars

Cytosolic invertase 1/2 (CINV1/2) irreversibly catalyzes Suc into glucose (Glc) and fructose (Frc) (Barratt et al., 2009). Here, we utilized the loss-of-function mutant of *CINV1/2*, *cinv1/2* (sugar signaling/metabolism mutant [Barratt et al., 2009; Meng et al., 2021]), to obtain the endogenous sugars of genetic manipulation.

The percentage of seedlings exhibiting cotyledon greening (greening rate) of the *cinv1/2* mutant (Figures S1A and S1C) substantially decreased as endogenous Glc content decreased (Figure S1D). These etiolated seedlings were grown under high white light (230 μmol quanta PAR m^{-2} s^{-1}) and no sugars. High white light conditions can provide a large amount of photosynthetic product (such as endogenous Suc). Further, the decrease in greening-seedling rate can be restored by the exogenous application of Glc but not Suc and Man (Figures S1B and S1C), probably because Suc and Man cannot be directly utilized. Suc is the substrate of CINV1/2, but Glc is the product of CINV1/2 (Barratt et al., 2009; Meng et al., 2020). Moreover, whereas Glc content declined in *cinv1/2* mutant seedlings under our conditions (Figure S1D), it was elevated in this mutant under other conditions (Lou et al., 2007; Barnes and Anderson, 2018). These findings suggested that decreasing Glc content in the *cinv1/cinv2* mutant interrupts signaling, which leads to blocked etiolated-seedling greening. Together, endogenous Glc may promote etiolated-seedling greening by signaling, but not metabolism.

To examine whether osmotic stress factors cause etiolated-seedling greening, we used the loss of vacuolar invertase 2 (VINV2) (*vinv2*, a sugar osmotic stress mutant; Sergeeva et al., 2006) to obtain the endogenous sugars of genetic manipulation. This mutant line exhibits considerably shorter roots and ~50% reduction in vacuolar invertase (Vac-Inv) activity compared with parental lines (Sergeeva et al., 2006). We examined etiolated-seedling greening in the *vinv2* mutant under high light and without sugars. Our findings indicated that whereas Glc content of the *vinv2* mutant evidently declined (Figure S1D), the

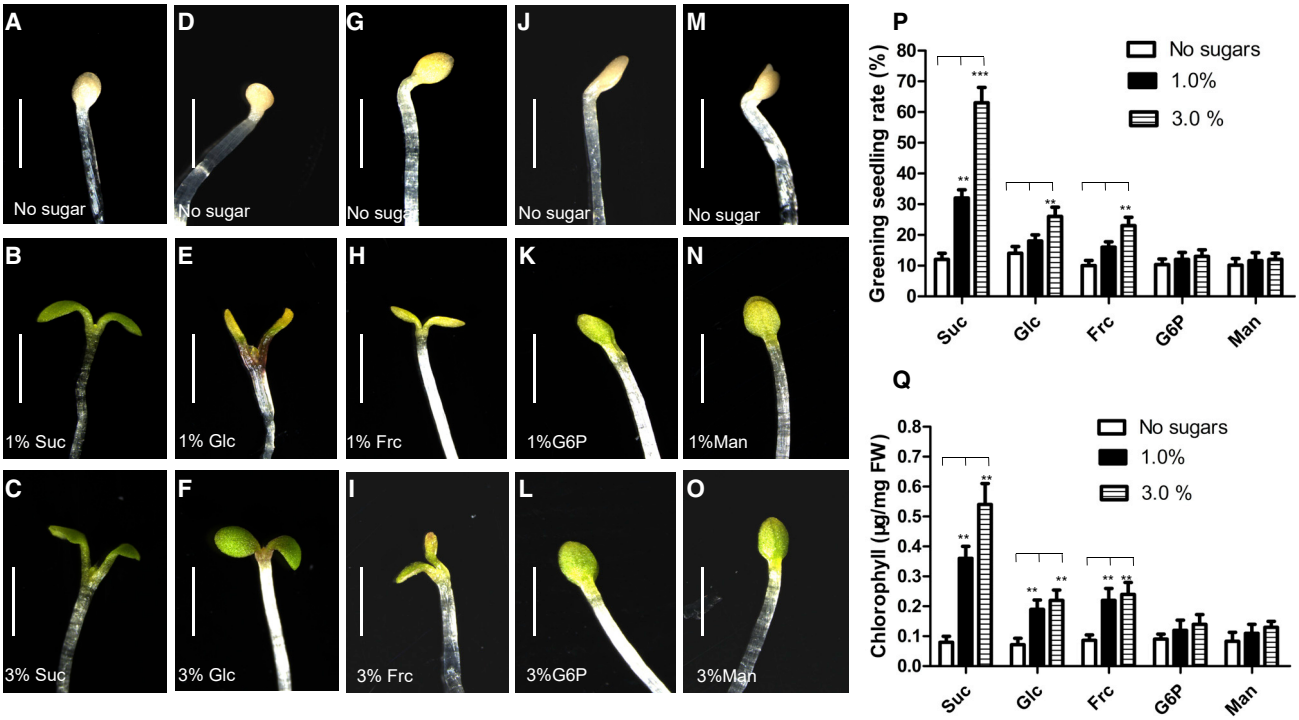

Figure 1. Suc preferentially facilitates the cotyledon greening of etiolated seedlings

(A–O) Images illustrating 8-day-old wild-type (Col-0) etiolated seedlings followed by 2 days of "median-level" white light irradiation (130 μmol quanta PAR m^{-2} s^{-1}) on solid MS medium with either 1% or 3% of sucrose (Suc), glucose (Glc), fructose (Frc), glucose-6-phosphate (G6P), and mannose (Man) or without sugar. Bar, 3 mm.

(P) Bar graph illustrating the greening rate of the given etiolated seedlings in (A)–(O).

(Q) Bar graph illustrating chlorophyll concentration of the given etiolated seedlings in (A)–(O).

Error bars represent SD (n = 46 in P; n = 3 in Q). Student's t test (***p < 0.001; **p < 0.01). See also Figure S1.

greening-seedling rate in this mutant was not different with wild-type seedlings (Figures S1A and S1C). These different Invs (cystolic invertase [Cinv-Inv] or Vac-Inv) caused the differential genetic phenotypes, indicating the importance of subcellular localization of invertases in signaling (Leskow et al., 2016). The Vac-Inv quantitative trait locus (QTL) influences both *Arabidopsis* carbon partitioning and biomass accumulation by a different regulation of Vac-Inv inhibitors at the mRNA level (Leskow et al., 2016). Therefore, that the loss of VINV2 lowered Glc content may block osmotic stress but not interrupt Glc signaling. Together, these findings confirmed that Glc may promote etiolated-seedling greening, but not metabolism, by signaling.

Taken together, the cotyledon greening of etiolated seedlings was promoted by endogenous Glc.

The cotyledon greening of etiolated seedlings was promoted preferentially by the exogenous application of Suc

While the endogenous sugar promoted etiolated-seedling greening (Figure S1), we have not provided evidence to identity whether exogenous sugars promote this process. To confirm and extend these observations, we performed the following experiments. With the increase of retention time under darkness, the capability of etiolated-seedling greening will gradually reduce (Zhong et al., 2009). We found that 8-day-old wild-type (Col-0) etiolated seedlings subjected to white light irradiation for 2 days was a desired time point to determine which of a few kinds of soluble sugars preferentially promote the cotyledon greening of etiolated seedlings.

We observed 8-day-old wild-type (Col-0) etiolated seedlings followed by 2 days of white light irradiation on solid MS medium without or with 1% and 3% Suc, Glc, Frc, glucose-6-phosphate (G6P), and mannose (Man). Under these conditions, the greening rate strikingly increased as the levels of exogenous Suc (but not Glc, Frc, G6P, and Man) increased (Figures 1A–1Q). This indicates that Suc exerts the most obvious positive effects on the cotyledon greening of etiolated seedlings. Frc and Glc also could stimulate cotyledon greening, but Man and G6P have no significant influences on the cotyledon greening. Therefore, in this work, we mainly focused on Suc affecting the cotyledon greening of etiolated seedlings.

Together, the cotyledon greening of etiolated seedlings was promoted preferentially by the exogenous application of Suc.

Suc preferentially induces *ACS7* expression and associated ET biosynthesis, which in turn promotes etiolated-seedling greening

Both ET production (Jeong et al., 2010) and etiolated-seedling greening (Figure 1) were preferentially induced by Suc relative to other sugars. ET promotes etiolated-seedling greening (Zhong

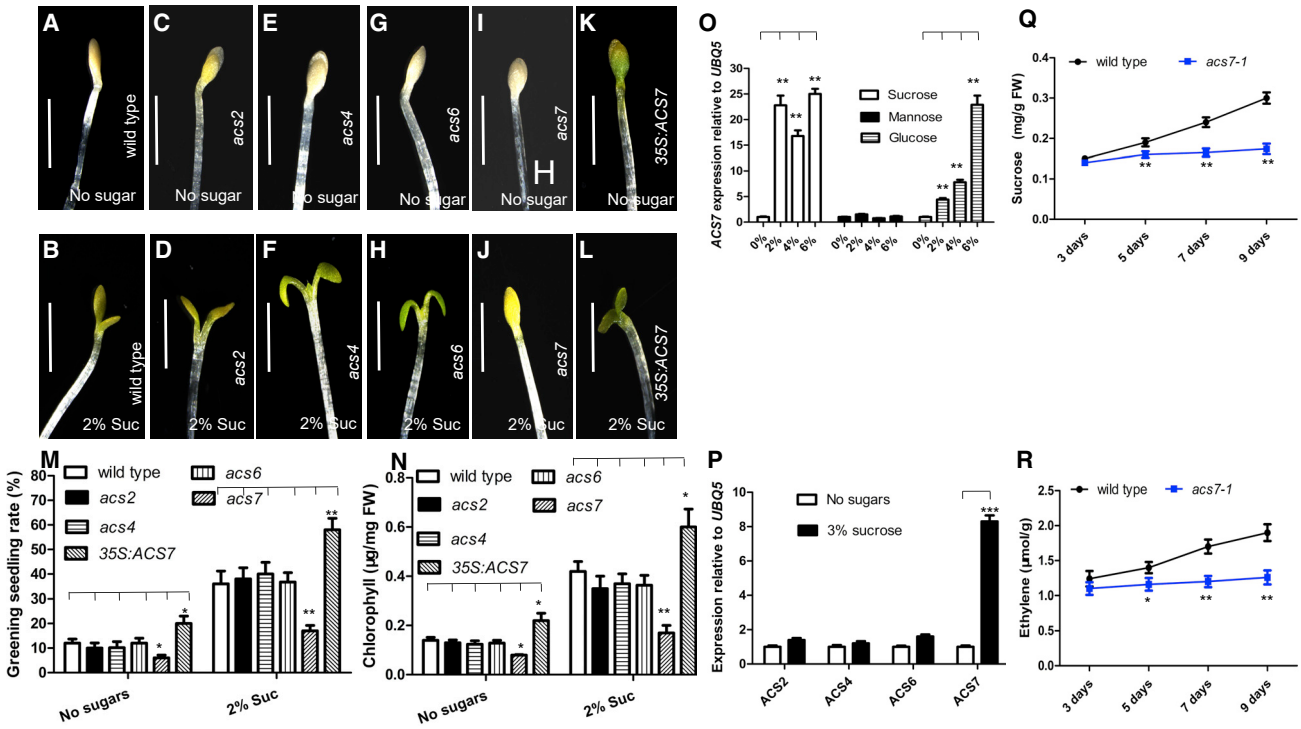

Figure 2. Suc promotes cotyledon greening by preferentially inducing *ACS7* expression and associated ethylene production

(A–L) Images illustrating 8-day-old wild-type (Col-0), *acs2*, *acs4*, *acs6*, *acs7*, and *35S:ACS7* etiolated seedlings followed by 2 days of median-level white light irradiation on solid MS medium with 2% Suc or without sugars. Bar, 3 mm.

(M) Bar graph illustrating the greening rate of the given etiolated seedlings in (A)–(L).

(N) Bar graph illustrating chlorophyll concentration of the given etiolated seedlings in (A)–(L).

(O) Bar graph illustrating *ACS7* expression in different exogenous Suc, Glc and Man. Eight-day-old wild-type etiolated seedlings were followed by 2 days of median-level white light irradiation. Subsequently, these seedlings were exposed to 0%, 2%, 4%, or 6% Suc, Glc, and Man for 30 min. The *ACS7* expression following exposure to 0% Suc, Glc, and Man is set as 1.

(P) Bar graph illustrating *ACS2*, *ACS4*, *ACS6*, and *ACS7* expression in the wild-type etiolated seedlings exposed to 3% Suc or no sugars for 1 h. Eight-day-old wild-type etiolated seedlings were followed by 2 days of median-level white light irradiation were used in this experiment. Quantification of the *ACS2*, *ACS4*, *ACS6*, and *ACS7* expression at no sugars is set as 1.

(Q and R) Bar graph illustrating Suc (Q) and ethylene (R) levels in 3-, 5-, 7-, and 9-day-old wild-type (Col-0) and *acs7-1* etiolated seedlings. The 2-, 4-, 6-, and 8-day-old wild-type (Col-0) and *acs7-1* etiolated seedlings were followed by 1 day of median-level white light irradiation.

Quantification was normalized to the expression of *UBQ5* in (O) and (P). Error bars represent SD (n = 44 in M; n = 3 in N–R). Student's t test (***$p < 0.001$; **$p < 0.01$; *$p < 0.05$). See also Figure S2.

et al., 2009). We therefore speculated whether Suc promotes etiolated-seedling greening by inducing the expression of genes encoding enzymes involved in ET biosynthesis. In this experiment, we employed a few loss-of-function mutants in *1-aminocyclopropane-1-carboxylate synthase* (*ACS*s), which encode key enzymes involved in ET biosynthesis (Liu and Zhang, 2004; Yoo et al., 2008). ACS2, ACS4, ACS6, and ACS7 are major factors of ET biosynthesis (Liu and Zhang, 2004; Yoo et al., 2008).

Genetic experiments revealed that the loss-of-function mutants of ACS2, ACS4, and ACS6, *acs2*, *acs4*, and *acs6*, were not significantly different from wild-type in the greening rate of etiolated seedling (Figures 2A–2H, 2M, and 2N). In contrast, whereas the loss-of-function of the *ACS7* mutant *acs7* (Figures S2A and S2B) reduced the greening rate, *ACS7* overexpression (*35S:ACS7*) (Figures S2A and S2B) elevated the greening rate relative to wild-type etiolated seedlings (Figures 2A, 2B, 2I, and 2N). This may result from a decline or an increase of 1-aminocyclopropane-1-carboxylic acid (ACC) or ET production in *acs7-1* or *35S:ACS7* seedlings, respectively, as ACC/ET promotes cotyledon greening (Zhong et al., 2009). Very recently, Xu et al. (2021) reported that ACS7, a key enzyme in ACC biosynthesis, has dual activities of ACC synthase, further suggesting that ACS7 may be a distinctive ACC synthase enzyme that is involved in the regulation of etiolated-seedling greening.

Consistent with these genetic data, molecular experiments presented that exogenous Suc, but not Glc and Man, preferentially induce *ACS7* expression (Figure 2O). Moreover, *ACS7* expression strikingly increased relative to *ACS2*, *ACS4*, and *ACS6* upon 3% Suc treatment (Figure 2P). Further, following exposure to white light for 1 day, 2-, 4-, 6-, and 8-day-old wild-type etiolated seedlings accumulated Suc and ET, with the accrual of these molecules increasing with seedling age (Figures 2Q and 2R). In contrast, the accumulation of Suc and ET in the *acs7* mutant had no significant difference during this time stage (Figures 2Q and 2R). These findings indicate that Suc/ET signaling-mediated cotyledon greening is partially dependent of ACS7 function.

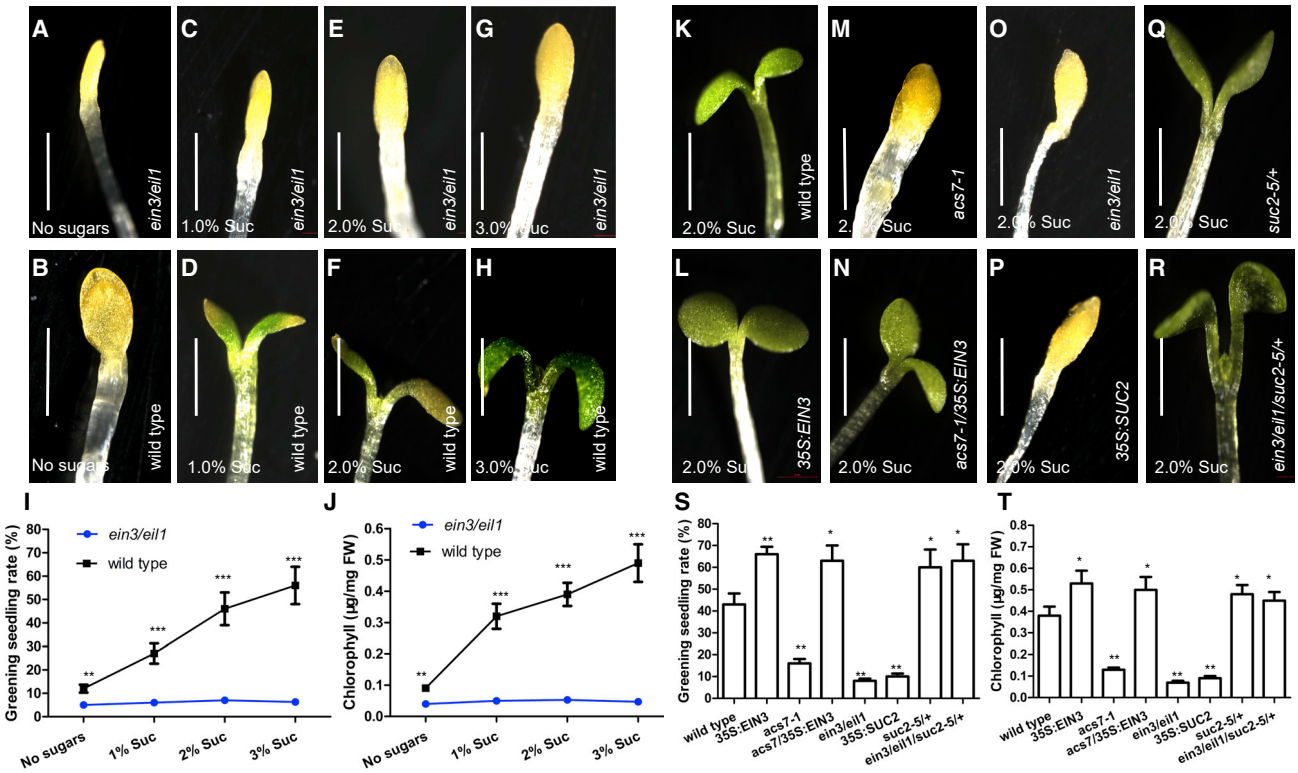

Figure 3. EIN3 acts downstream and upstream of ACS7 and SUC2 in the regulation of Suc signaling-mediated cotyledon greening of etiolated seedlings, respectively

(A–H) Images illustrating 8-day-old wild-type (Col-0) and *ein3/eil1* etiolated seedlings followed by 2 days of median-level white light irradiation on solid MS medium with 1%, 2%, or 3% of Suc or without sugar. Bars, 4 mm.

(I) Bar graph illustrating the greening rate of the given etiolated seedlings in (A)–(H).

(J) Bar graph illustrating chlorophyll concentration of the given etiolated seedlings in (A)–(H).

(K–R) Images illustrating 8-day-old wild-type (Col-0) (K), *35S:EIN3* (L), *acs7-1* (M), *acs7-1/35S:EIN3* (N), *ein3/eil1* (O), *35S:SUC2* (P), *suc2-5*/+ (Q), and *ein3/eil1/suc2-5*/+ (R) etiolated seedlings followed by 2 days of median-level white light irradiation on solid MS medium with 2% Suc. Bar, 1.0 mm.

(S) Bar graph illustrating the greening rate of the given etiolated seedlings in (K)–(R).

(T) Bar graph illustrating chlorophyll concentration of the given etiolated seedlings in (K)–(R).

Error bars represent SD (n = 43 in I and S; n = 3 in J and T). Student's t test (***$p < 0.001$; **$p < 0.01$; *$p < 0.05$). See also Figure S2.

In aggregate, our data reveal that Suc preferentially induces *ACS7* expression and associated ET biosynthesis, which in turn promotes etiolated-seedling greening.

Suc/ET signaling-mediated cotyledon greening is partially dependent of EIN3/EIL1 acting downstream of ACS7

Suc drives etiolated-seedling greening by preferentially inducing *ACS7* expression and associated ET biosynthesis (Figure 2), and induced ET activates a key ET component, EIN3, by its canonical signal transduction pathway (Cho et al., 2006; Binder et al., 2007) to promote ET-mediated etiolated-seedling greening (Zhong et al., 2009). Therefore, we determined if EIN3 might be a component integral to the developmental process of Suc/ET signaling-mediated etiolated-seedling greening. The close paralogs EIN3 and EIN3-like 1 (*EIL1*) have redundant functions (Cho et al., 2006; Binder et al., 2007). Thus, we determined whether *EIN3/EIL1* participates in the regulation of Suc/ET signaling-mediated etiolated-seedling greening.

The greening rate of 8-day-old wild-type (Col-0) etiolated seedlings subjected to white light irradiation for 2 days on MS medium without or with 1%, 2%, or 3% Suc was significantly elevated with the increase of exogenous Suc concentrations. By contrast, under the same conditions, *ein3/eli1* seedlings exhibited no obvious difference in greening rate in response to different Suc concentrations (Figures 3A–3J). These findings indicate that Suc/ET signaling-mediated etiolated-seedling greening is dependent of EIN3/EIL1 function.

To extend these data, we determined the consequence of *EIN3* overexpression on Suc/ET signaling-mediated etiolated-seedling greening. A *35S:EIN3* in the wild-type background showed increased greening seedling rate relative to wild-type plants (Figures 3K, 3L, 3S, and 3T). This observation contrasted with that of the *acs7-1* mutant defective in ET biosynthesis, which exhibited reduced greening-seedling rate (Figures 3K, 3M, 3S, and 3T). Further, we crossed the *35S:EIN3* transgene to the *acs7-1* mutant and determined the rate of seedling greening in the resulting *acs7-1/35S:EIN3* line (Figure S2B). This line produced a greening rate similar to the *35S:EIN3* line

(Figures 3K, 3L, 3N, 3S, and 3T). These findings indicate that ACS7 acts upstream of EIN3 to positively regulate Suc/ET signaling-mediated etiolated-seedling greening.

Collectively, these findings show that Suc/ET signaling-mediated cotyledon greening is partially dependent on EIN3/EIL1 acting downstream of ACS7.

EIN3 represses *SUC2* expression

Chromatin immunoprecipitation sequence (ChIP-seq) analysis of EIN3 (Chang et al., 2013) indicated that EIN3 may directly regulate *SUC4* expression. Further, phloem transport is promoted in response to light cues, and sugar export from sinks is directly linked to SUC activity (Xu et al., 2018). In this context, *SUC2* is a major transporter of Suc during phloem loading in *Arabidopsis* (Kühn et al., 1997; Srivastava et al., 2009). As we identified the transcriptional regulator EIN3 as a key component in Suc/ET-signaling etiolated-seedling greening (Figure 3), we therefore explored if transcription factor EIN3 could directly interact with *SUC2* promoter sequences to regulate *SUC2* expression and, by extension, Suc transport.

While it is well established that EIN3 protein levels are enhanced with increasing seedling age (Li et al., 2013), our data revealed that *SUC2* transcripts declined with age and were of greater abundance in *ein3/eil1* seedlings relative to wild-type ones (Figure S3C). This result was further supported by the upregulation of *SUC2* expression in *ein3/eil1* seedlings (Jeong et al., 2010). Further, transient expression experiments in *Nicotiana benthamiana* showed that coexpression of *EIN3* decreased the expression of a *SUC2* promoter-reporter gene, *ProSUC2:LUCIFERASE* (*LUC*) (Figures S3A and S3B). Thus, these findings suggest that EIN3 inhibits *SUC2* expression.

ET suppression of *SUC2* expression may be partially dependent of EIN3 function

To determine whether *SUC2* expression is sensitive to transiently applied ET, we monitored *SUC2* expression over time in response to the exogenously supplied ET precursor ACC. Informatively, *SUC2* expression decreased after ACC application. Further, *SUC2* transcripts remained suppressed 60 min after ACC treatment of wild-type plants (Figure S3D). Conversely, there was no obvious suppression of *SUC2* expression in *ein3/eil1* seedlings (Figure S3D). We also monitored *SUC2* expression over time in response to either an exogenously supplied ET synthesis inhibitor, aminoethoxyvinylglycine (AVG), or an ET-binding inhibitor, silver (Jeong et al., 2010). *SUC2* expression was significantly elevated after application of either AVG or silver (Figures S3E and S3F). Moreover, *SUC2* transcripts remained strikingly elevated at 60 min post treatment in wild-type plants, but this elevation was not detected in *ein3/eil1* seedlings (Figures S3E and S3F).

In sum, these data indicate that ET suppression of *SUC2* expression may be partially dependent on EIN3 function.

EIN3 directly binds to the *SUC2* promoter

Examination of DNA sequences comprising the *SUC2* promoter revealed putative EIN3 binding sites (EBSs) (Li et al., 2013) (Figure 4A). To explore whether EIN3 can interact with any of these EBSs, we employed a transgenic *Arabidopsis* line possessing an *EIN3pro:EIN3-GFP* line (Figure S2C). We thus performed ChIP analysis to determine whether EIN3 bound directly to *SUC2* promoter sequences. Indeed, EIN3 strongly bound to one *SUC2* promoter sequence (S2), which contained a single EBS, but not to three other *SUC2* promoter sequences (S1, S3, or S4) (Figure 4B). Moreover, ET treatment enhanced EIN3 binding to S2 of the *SUC2* promoter (Figure 4C), likely because ET is known to enhance EIN3 stability or activity (Yanagisawa et al., 2003). In addition, EIN3 association with sequence S2 in the *SUC2* promoter increased over time in *EIN3pro:EIN3-GFP* seedlings (Figure 4D), possibly because EIN3 stability or activity was enhanced with increasing seedling age (Li et al., 2013). This association was strongly correlated with a decline in *SUC2* expression with increasing age (Figure S3A), which may be because with increasing seedling age, the increase of EIN3 association with sequence S2 (Figure 4D) inhibits *SUC2* expression.

Further, A *SUC2* promoter construct containing a mutated EBS (*mEBS*), *SUC2(mEBS)pro::SUC2*, was transformed into a *suc2-5* line expressing *35S:EIN3-GFP* [*35S:EIN3-GFP/SUC2(mEBS)pro::SUC2/suc2-5*]. The absence of an intact EBS within the S2 sequence of the *SUC2* promoter construct decreased EIN3 binding (Figure 4E). Significantly, the seedling-greening rate of the *35S:EIN3-GFP/SUC2(mEBS)pro::SUC2/suc2-5* seedlings was reduced compared with the *35S:EIN3-GFP/ein3/eil1* seedlings (Figures 4F and 4G), suggesting that EIN3 binding to the *SUC2* promoter is required to suppress SUC2 function and that its impairment blocks etiolated-seedling greening. Taken together, our findings indicate that EIN3 directly binds to the promoter of the *SUC2* gene *in vivo* to inhibit *SUC2* expression.

To determine if EIN3 can bind directly to the S2 EBS within the *SUC2* promoter *in vitro*, we performed an electrophoretic mobility shift assay (EMSA). EIN3 bound exclusively to the labeled S2 EBS element *in vitro* (Figure 4H). Excess unlabeled competitor DNA effectively abolished this binding ability in a dose-dependent manner, thereby establishing the specificity of this binding (Figure 4H). We confirmed and extended these findings by determining that mutant S2 DNA sequences cannot abolish EIN3 binding to the labeled S2 EBS element *in vitro* (Figure 4I).

Together, these data indicate that EIN3 directly binds to the *SUC2* promoter to suppress *SUC2* expression *in vivo* and *in vitro*.

SUC2 acts genetically downstream of *EIN3*, repressing etiolated-seedling greening

The homozygous *SUC2* loss-of-function *suc2-5*/– mutant is a null allele (Figure S2E); it is well established that these seedlings exhibit severely retarded growth, so seedlings of this line were not viable (Lei et al., 2011). We therefore utilized a heterozygote *suc2-5*/+ mutant to explore cotyledon greening. Eight-day-old etiolated *suc2-5*/+ seedlings (Figure S2E) grown on solid MS medium with 2% Suc subjected to white light irradiation for 2 days promoted etiolated-seedling greening (Figures 3K, 3Q, 3S, and 3T). In contrast, a *35S:SUC2* transgenic line (Figure S2D) failed to show etiolated-seedling greening (Figures 3K, 3P, 3S, and 3T). Thus, *SUC2* negatively regulates the cotyledon greening of etiolated seedlings.

Subsequently, we analyzed the genetic interactions between *EIN3* and *SUC2*. The generated *ein3/eil1/suc2-5*/+ line (Figure S2F) exhibited accelerated seedling greening compared

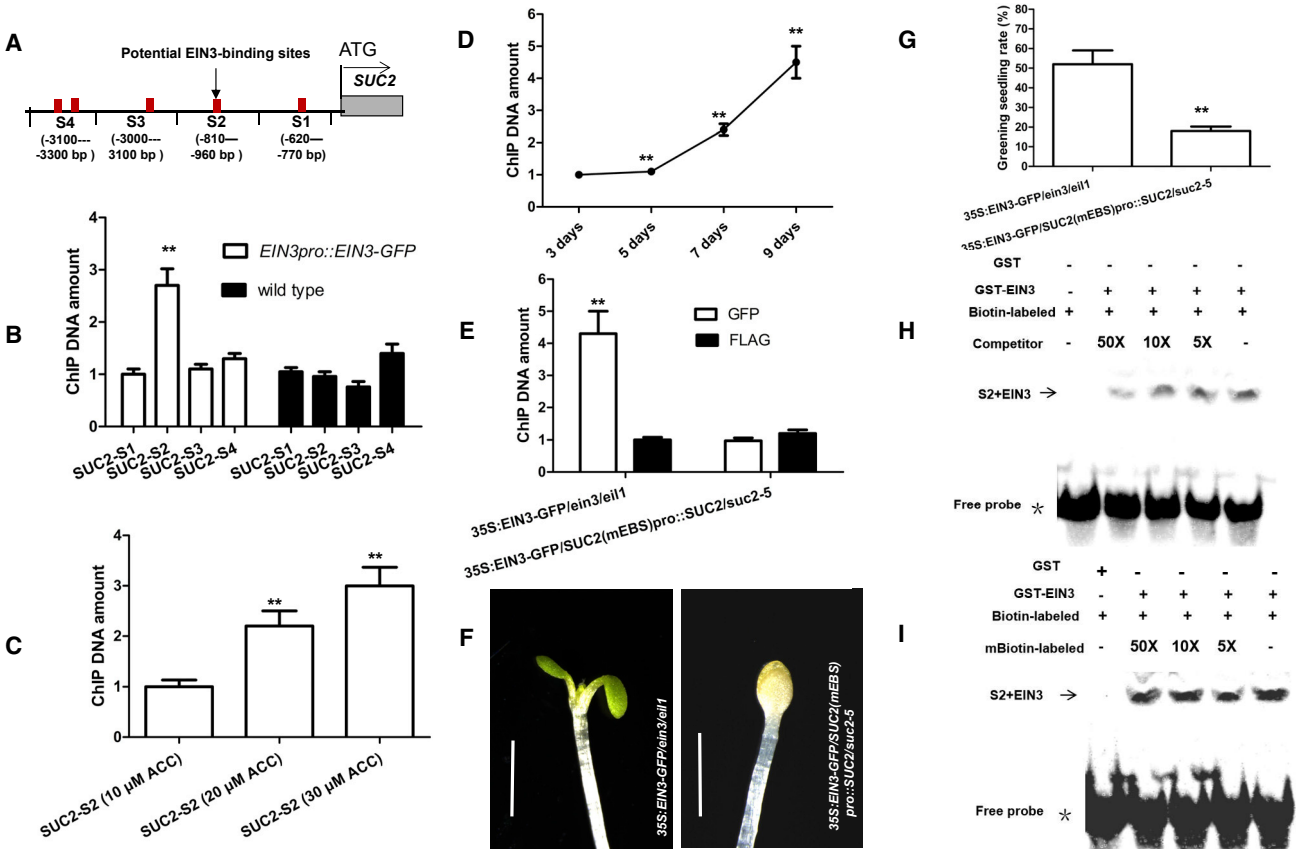

Figure 4. EIN3 directly interacts with and supresses the *SUC2* promoter

(A) Schematic of the *SUC2* promoter subjected to ChIP-qPCR analysis.

(B) Bar graph illustrating ChIP-qPCR. Eight-day-old *EIN3pro::EIN3-GFP* and wild-type etiolated seedlings were followed by 2 days of median-levle white light irradiation on MS medium with 1% Suc. Protein extracts were from these seedlings. Particular chromatin regions of *SUC2* promoter were enriched using an anti-GFP antibody, as detected by real-time PCR analysis. Quantification in *SUC2-S1* was set as 1.

(C) Bar graph illustrating ChIP-PCR. Eight-day-old *EIN3pro::EIN3-GFP* etiolated seedlings were followed by 2 days of median-level white light irradiation on MS medium with 1% Suc. Subsequently, these *EIN3pro::EIN3-GFP* seedlings were treated with 10, 20, and 30 μM ACC for 30 min. Protein extracts were from these seedlings. Particular chromatin regions (S2) of *SUC2* promoter were enriched by using an anti-GFP antibody. Quantification of the ChIP DNA amount at 10 μM ACC for 30 min was set as 1.

(D) Bar graph illustrating ChIP-PCR over time. The 3-, 5-, 7-, and 9-day-old *EIN3pro::EIN3-GFP* seedlings were used as ChIP-qPCR materials. These seedlings were from 2-, 4-, 6-, and 8-day-old *EIN3pro::EIN3-GFP* etiolated seedlings followed by 1 day of median-level white light irradiation on MS medium with 1% Suc. Particular chromatin regions (S2) of *SUC2* were enriched by using an anti-GFP antibody. Quantification of 3-day-old *EIN3pro::EIN3-GFP* seedlings was set as 1.

(E) Bar graph illustrating ChIP-qPCR in S2 mutation. Ten-day-old *35S:EIN3-GFP/SUC2(mEBS)pro::SUC2/suc2-5* or *35S:EIN3-GFP/ein3/eil1* seedlings were used as ChIP-qPCR materials. These seedlings were from 8-day-old *35S:EIN3-GFP/SUC2(mEBS)pro::SUC2/suc2-5* or *35S:EIN3-GFP/ein3/eil1* etiolated seedlings followed by 2 days of median-level white light irradiation on MS medium with 1% Suc. ChIP was performed to analyze the *in vivo* interaction between EIN3 and the S2 sequence mutation of the *SUC2* promoter. Particular chromatin regions of S2 sequence mutation within the *SUC2* promoter were enriched using an anti-GFP antibody, as detected by qPCR analysis. Anti-FLAG antibody was used as a control. Quantification of 10-day-old *35S:EIN3-GFP/ein3/eil1* seedlings was set as 1.

(F) Images illustrating of 8-day-old *35S:EIN3-GFP/SUC2(mEBS)pro::SUC2/suc2-5* or *35S:EIN3-GFP/ein3/eil1* etiolated seedlings followed by 2 days of white normal light irradiation on solid MS medium with 1% Suc. Bars, 3.0 mm.

(G) Bar graph illustrating the greening rate of the given etiolated seedlings in (F).

(H) Images illustrating the unlabeled *SUC2* promoter sequence were used as a competitor to determine the specificity of DNA-binding activity for EIN3.

(I) Images illustrating a mutant version of the promoter of *SUC2* were labeled with biotin and used for EMSA with EIN3 polypeptides. Free probe and EIN3 probe complexes are indicated by an asterisk and arrows, respectively, in (H) and (I).

Quantifications were normalized to the expression of *UBQ5* in (B)–(E). Error bars represent SD (n = 3 in B–E; n = 38 in G). Student's t test (**p < 0.01). See also Figures S2 and S3.

with the wild-type line. This result was similar to that obtained with the *suc2-5*/+ line (Figures 3K and 3O–3T). Thus, *SUC2* acts genetically downstream of *EIN3*/*EIL1* to block etiolated-seedling greening.

The ACS7–EIN3–SUC2 module is located on phloems of cotyledons

In *Arabidopsis*, *SUC2* encodes a proton/Suc symporter localized throughout collection and transport phloem; thus, SUC2 is

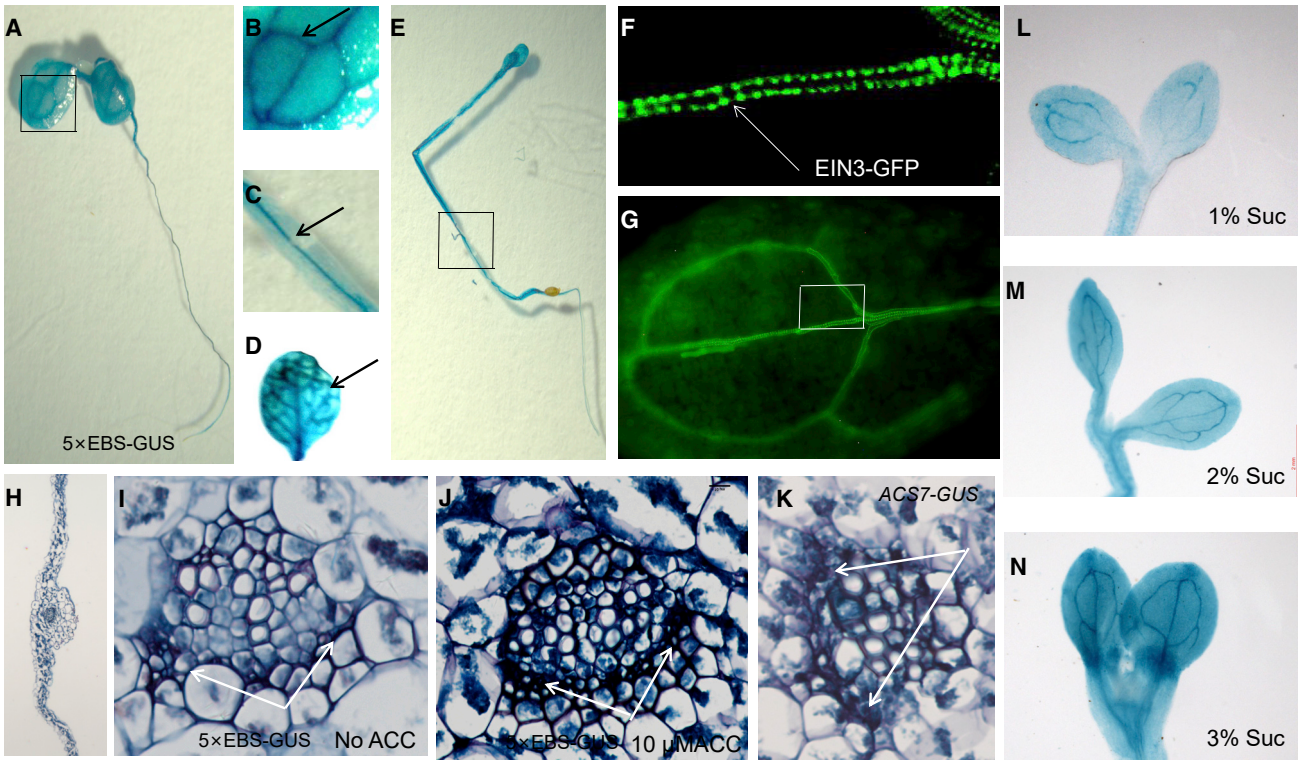

Figure 5. EIN3 activity and EIN3 protein accumulation in the vascular bundle

(A–E) Developmental expression of a *5×EBS* (*EIN3 binding site*)*-GUS* transgene in seedlings.

(B) Amplified square from (A).

(C) is amplified from (D).

(E) *EBS-GUS* etiolated seedlings were grown on MS medium with 1% Suc under darkness for 6 days.

(F and G) *35S:EIN3-GFP* seedlings were grown on MS medium with 2% Suc for 7 days, and their cotyledons were observed under a fluorescence microscope. (F) is the amplified square indicated in (G). Arrows indicate sieve tubes and companion cells within the phloem.

(H–J) Parafin sections of leaf blades. Arrows indicate sieve tubes and companion cells in the phloem in (I) and (J). Seven-day-old wild-type (Col-0) etiolated seedlings grown on MS medium with no ACC (I) or 10 μM ACC (J) were followed by 2 days of white median-level light irradiation.

(K) *ACS7pro-GUS* expression in cotyledons. Arrows indicate sieve tubes and companion cells within the phloem.

(L–N) Five-day-old *5×EBS-GUS* etiolated seedlings subjected to white light irradiation for 1 day were grown on solid MS medium with either 1% or 3% Suc or in the absence of sugar.

See also Figures S4 and S7.

essential for the effective transport of Suc from source to sink tissues (Stadler et al., 1995; Srivastava et al., 2009). Building on our findings, we therefore determined if the ACS7-EIN3-|SUC2 module might be located on phloems of cotyledons.

To observe the location of the ACS7-EIN3-|SUC2 module on phloems of cotyledons, we firstly employed a transgenic line containing the β-glucuronidase (*GUS*) reporter gene downstream of five tandem repeats of an EBS (*5×EBS*:*GUS*), which was utilized to monitor EIN3 binding activity (Li et al., 2013). EIN3 activity was observed in the veins of cotyledons, true leaves, and hypocotyls either under white light or in darkness (Figures 5A–5E). EIN3 activity was also detected in sieve tubes and in companion cells in phloems (Figures 5H–5J). EIN3 binding activity revealed by GUS staining was elevated with increasing ACC (Figures 5I and 5J), suggesting an increase in EIN3 binding to its cognate EBS and, by extension, a localization of ET accumulation during etiolated-seedling greening. Further, when Suc levels were increased, EIN3 binding activity was enhanced together with the cotyledon greening of the *5×EBS-GUS* line (Figures 5L–5N), suggesting that Suc-signaling-induced ET promotes cotyledon greening by the ACS7-EIN3-|SUC2 module.

Employing the *EIN3pro:EIN3-GFP* line to report EIN3 abundance and localization, EIN3 was located primarily within the phloem sieve tube elements and companion cells (Figures 5F and 5G), congruent with SUC2 (Stadler et al., 1995; Kühn et al., 1997; Srivastava et al., 2008, 2009). Further, previous findings showed that ACS7, integral to ET biosynthesis, promotes vascular cambium development in *Arabidopsis* (Yang et al., 2020), suggesting that ACS7 function may regulate the development of phloem sieve tube elements and associated companion cells. In agreement with this posit, our data indicate that an *ACS7* promoter driving expression of a GUS reporter gene (*ACS7pro-GUS*) generated strong GUS activity within phloem sieve tube elements and associated companion cells (Figure 5K).

Taken together, these findings indicate that the ACS7–EIN3–|SUC2 module is located on phloems of cotyledons.

The ACS7–EIN3–|SUC2 module mediates the phloem loading of Suc in cotyledons

To further elucidate the mechanism by which the ACS7–EIN3–|SUC2 module mediates Suc phloem loading, a [^{14}C] Suc phloem loading assay was performed. Our findings revealed that the rate of Suc phloem loading in the cotyledons of wild-type, *acs7-1*, *ein3/eil1*, *suc2-5*/+, *35S*:*SUC2*, *35S*:*EIN3*, and *35S:ACS7* seedlings was remarkably different (Figure S4A). The phloem-loading rate was significantly increased in *acs7-1*, *ein3/eil1*, and *35S*:*SUC2* seedlings. In contrast, this rate decreased in *suc2-5*/+ *35S*:*EIN3*, and *35S:ACS7* lines (Figure S4A). These findings thus indicate that the ACS7-EIN3-|SUC2 module suppresses Suc transport in the phloem cell of cotyledons.

Further, we assayed the Suc contents of cotyledons (source tissues) and shoot apexes (sink tissues) in 9-, 11-, and 13-day-old wild-type, *acs7-1*, *suc2-5*/+, and *ein3/eil1* seedlings exposed to white light for 5 and 10 h, respectively. In all seedlings, Suc accumulation increased in both source and sink tissues with increasing seedling age (Figures S4B and S4C), suggesting that phloem loading of Suc results in typical Suc distributions in both source and sink tissues. Moreover, after white light exposure for 5 h, Suc accumulation decreased over time in *acs7-1* and *ein3/eil1* cotyledons but increased in *suc2-5*/+ cotyledons compared with that of wild-type (Figure S4B). Consistent with this, the phloem-loading rate of Suc in cotyledons increased over time in *acs7-1* and *ein3/eil1* cotyledons but decreased in *suc2-5*/+ cotyledons compared with that of wild-type (Figure S4A). As a result, after light exposure for 10 h, Suc accumulation increased over time in the shoot apex of *acs7-1* and *ein3/eil1* plants but decreased in the shoot apex of the *suc2-5*/+ line compared with that of wild-type plants (Figure S4C). These data were strongly correlated with a decline in *SUC2* expression with increasing age (Figure S4A), and with increasing seedling age, the increase of EIN3 association with sequence S2 (Figure 4D) inhibits *SUC2* expression. Although Suc contents in sink leaves were substantially altered in *acs7-1*, *suc2-5*/+, and *ein3/eil1* seedlings compared with those of wild-type, Glc contents were not evidently different between wild-type and mutant sink leaves (Figure S4D), suggesting that the ACS7-EIN3–SUC2 module only affects Suc accumulation. Similar to this, in potato plants, Suc content in sink leaves (such as shoot apical meristems) was examined at different developmental stages. Whereas the levels of Fru and Glc in sink leaves were not obviously altered between transgenic and wild-type plants, the contents of Suc differ conspicuously (Chincinska et al., 2008).

In sum, these findings indicated that under darkness, the ACS7–EIN3–|SUC2 module inhibits Suc export from cotyledons and thus accumulates Suc in cotyledons (source tissues) by suppressing the phloem loading of Suc in cotyledons.

EIN3 inhibits *phyA* expression

Far-red light has been shown to block etiolated-seedling greening by a *phyA*-dependent pathway, which can be restored by the application of exogenous Suc (Barnes et al., 1996). ChIP-seq analysis of EIN3 (Chang et al., 2013) has previously revealed that EIN3 might directly regulate *phyA* expression. Therefore, we determined whether *phyA* might be a downstream target gene of EIN3.

Results from a time course qPCR analysis revealed that *phyA* transcripts decreased with age and, over time, were higher in *ein3/eil1* than in wild-type seedlings (Figure S5A). However, EIN3 accumulated with increasing age (Li et al., 2013). This suggests that EIN3 might inhibit *phyA* expression. Further, we employed transient expression analysis in *N. benthamiana*. Coexpression of *EIN3* together with a *phyA* promoter driving the expression of a *LUC* reporter gene established that EIN3 suppressed expression from the *phyA* promoter (Figures 6A and 6B). These findings indicate that EIN3 inhibits *phyA* expression and that *phyA* may be a downstream target gene of EIN3.

ET suppression of *phyA* expression may be partially dependent of EIN3 function

To explore whether *phyA* expression is sensitive to transiently applied ET, we monitored *phyA* expression over time in response to the exogenously supplied ET precursor ACC. *phyA* expression decreased 60 min after treatment of the wild-type line, but this was not the case in *ein3/eil1* double mutant seedlings (Figure S5B). Furthermore, we monitored *phyA* expression over time in response to the exogenously supplied ET synthesis inhibitors AVG and silver. *phyA* expression increased after application of either AVG or silver and remained highly elevated 60 min after the treatment of wild-type but not *ein3/eil1* seedlings (Figures S5C and S5D). This suggests that ET, induced by accumulated Suc in germinating seeds under darkness, appears to promote etiolated-seedling greening, likely by EIN3 transcriptional suppression of *phyA*, a negative regulator of etiolated-seedling greening, following white light illumination.

Together, ET suppression of *phyA* expression may be partially dependent on EIN3 function.

EIN3 directly binds to *phyA* promoter

Our observations prompted us to determine whether EIN3 directly regulates *phyA* transcription. Examination of the *phyA* promoter revealed the presence of a putative EBS (TTCAAA [or its complementary TTTGAA]) (Li et al., 2013). For subsequently analysis, we designated *phyA* promoter sequences as P1 or P2 (Figure 6C). The DNA sequences within the *phyA* promoter were utilized for ChIP analysis together with *EIN3pro:EIN3-GFP* transgenic seedlings (Figure 6C). DNA primers located within the P1 region of the *phyA* promoter (Figure 6C) produced transcripts of the greatest abundance (Figure 6D). Furthermore, EIN3 association with the P1 sequence in the *phyA* promoter increased over time in *EIN3pro:EIN3-GFP* seedlings (Figure 6E). In contrast, a *phyA* promoter containing mutations within the EBS (*phyA*(*mEBS*)*pro::phyA*) displayed reduced EIN3 binding within the P1 region of the *phyA* promoter (Figure 6F).

Subsequently, EMSA was performed to determine whether EIN3 can directly bind to the *phyA* promoter P1 sequence *in vitro*. Indeed, the recombinant EIN3 protein bound to the labeled P1 element *in vitro* (Figure 6G). Excessive amounts of the unlabeled competitor P1 DNA sequence effectively abolished this binding in a dose-dependent manner (Figure 6G). Further, excessive amounts of the mutated competitor mP1 DNA did not induce effective binding in a dose-dependent manner (Figure 6H). Our data indicates that EIN3 directly binds to the *phyA* promoter

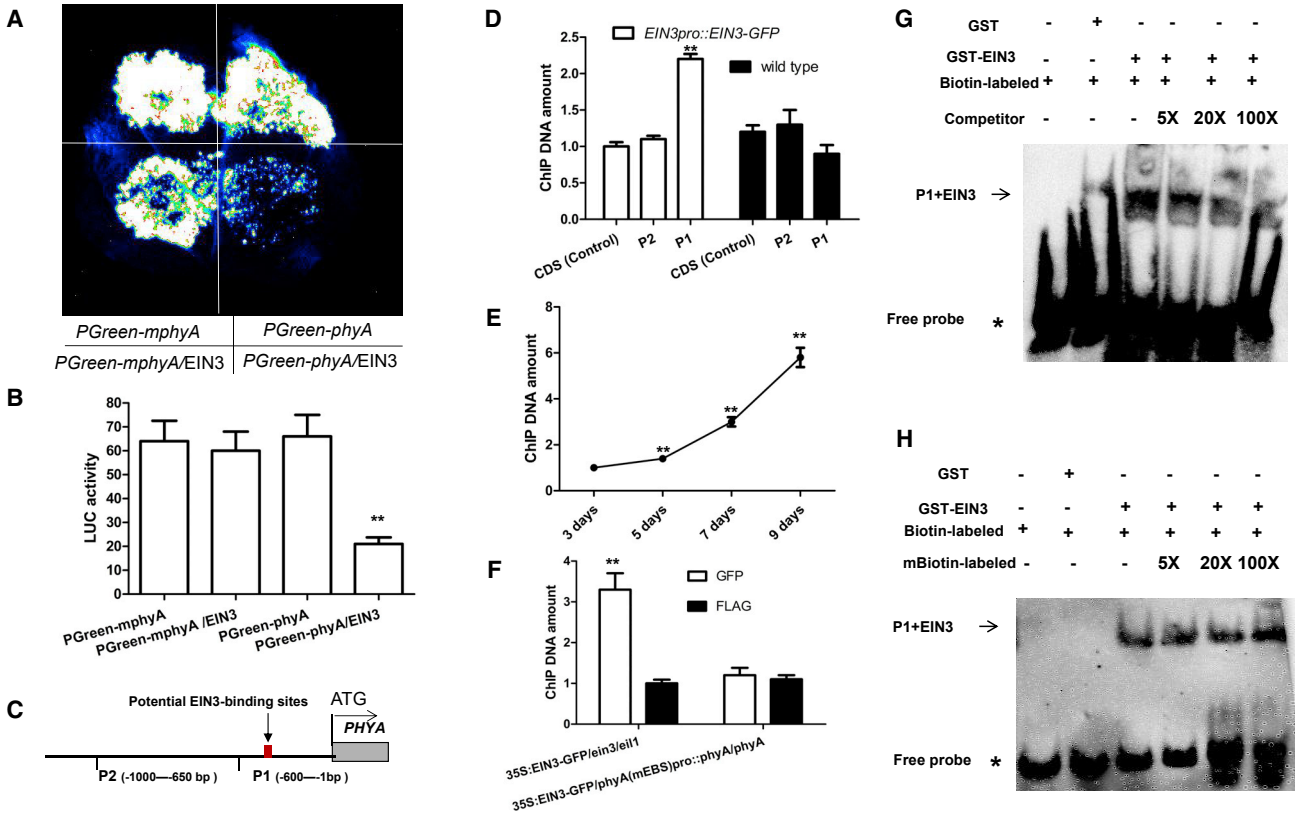

Figure 6. EIN3 directly interacts with the *phyA* promoter to suppress *phyA* expression

(A) Images illustrating transient expression of the 35S:EIN3 effector construct in conjunction with the *phyApro- LUC* reporter construct in *N. benthamiana* leaves. Note: *PGreen-mphyA* indicates that the conserved sites (TTCAAA) of the P1 region within the *phyA* promoter were mutated.

(B) Bar graph illustrating luminescence units are represented by LUC activity.

(C) Schematic of the promoter of *phyA* used for ChIP analysis.

(D) Bar graph illustrating ChIP-qPCR analysis. Eight-day-old *EIN3pro::EIN3-GFP* etiolated seedlings were followed by 2 days of median-level white light irradiation on MS medium with 1% Suc. Using these seedlings as ChIP-qPCR materials, particular chromatin regions of *phyA* promoter were enriched using an anti-GFP antibody, as detected by real-time PCR analysis. The coding sequence (CDS) was set as 1.

(E) Bar graph illustrating ChIP-PCR over time. The 3-, 5-, 7-, and 9-day-old *EIN3pro::EIN3-GFP* seedlings were from 2-, 4-, 6-, and 8-day-old *EIN3pro::EIN3-GFP* etiolated seedlings followed by 1 day of median-level white light irradiation on MS medium with 1% Suc. Using these seedlings as ChIP-qPCR materials, particular chromatin regions (P1) of the *phyA* promoter were enriched using an anti-GFP antibody, as detected by qPCR analysis. Quantification of 3-day-old *EIN3pro::EIN3-GFP* seedlings was set as 1.0.

(F) Bar graph illustrating ChIP-qPCR in S2 mutation. Ten-day-old *35S:EIN3-GFP/phyA(mEBS)pro::phyA/suc2-5* or *35S:EIN3-GFP/ein3/eil1* seedlings were used as ChIP-qPCR materials. These seedlings were from 8-day-old *35S:EIN3-GFP/phyA(mEBS)pro::phyA/suc2-5* or *35S:EIN3-GFP/ein3/eil1* etiolated seedlings followed by 2 days of "median level" white light irradiation on MS medium with 1.0% Suc. ChIP was performed to analyze the *in vivo* interaction between EIN3 and the P1 sequence mutation of the *phyA* promoter. Particular chromatin regions of P1 within the *phyA* promoter were enriched using anti-GFP antibody, as detected by qPCR analysis. Anti-FLAG antibody was used as a control. Quantification of 10-day-old *35S:EIN3-GFP/ein3/eil1* seedlings was set as 1.0.

(G) Images illustrating the unlabeled *phyA* promoter was used as a competitor to determine the specificity of DNA-binding activity for EIN3.

(H) Images illustrating a mutant version of the promoter of *phyA* was labeled with biotin and used for EMSA with EIN3 polypeptides.

Free probe and EIN3 probe complexes are indicated by an asterisk and arrow, respectively, in (G) and (H). Quantification was normalized to the expression of *UBQ5* in (D)–(F). Error bars represent SD (n = 3 in D–F; n = 5 in B). Student's t test (**p < 0.01 in B and D–F). See also Figures S5 and S6.

to suppress *phyA* expression, further indicating that *phyA* is the downstream target gene of EIN3.

Taken together, these findings reveal that EIN3 directly binds to the *phyA* promoter to inhibit *phyA* expression *in vivo* and *in vitro*.

phyA acts genetically downstream of *EIN3* to inhibit etiolated-seedling greening

We further analyzed the genetic interactions between *EIN3* and *phyA*. Despite the absence of *phyA* function, etiolated-seedling greening was promoted in the *phyA* mutant line, whereas greening of *ein3/eil1* seedlings was considerably reduced compared with that of wild-type seedlings (Figure S6). Moreover, in an *ein3/eil1/phyA* triple mutant line, etiolated-seedling greening was similar to that of the *phyA* line (Figure S6).

Taken together, therefore, *phyA* acts genetically downstream of *EIN3/EIL1* to negatively regulate etiolated-seedling greening.

DISCUSSION

The switch from skotomorphogenesis to photomorphogenesis is indispensable for seedling survival and development. Integral to this process is etiolated-seedling greening, where the onset of illumination initiates an etioplast-to-chloroplast transition. While sugars have long been shown to affect etiolated-seedling greening, the underpinning molecular mechanisms have remained elusive. Further, whereas the mechanical stress of the soil has been reported to activate ET production to promote cotyledon greening by a key ET component, EIN3, controlling a few phytochrome and associated factors, how this mechanical stress induces ET production remains unclear.

Previous reports have demonstrated that *Arabidopsis* and tomato grown under continuous far-red light cannot generate chlorophyll and fail to turn green when subsequently exposed to continuous white light (Barnes et al., 1996). A follow-up study revealed that continuous far-red light irradiation results in the failure of *Arabidopsis* to turn green because aberrant plastids form in the developing cotyledons (Barnes et al., 1996). A functional PHYA is essential for this physiological process (Barnes et al., 1996), which is repressed when seedlings are grown on a Suc-containing medium. However, the molecular mechanisms by which Suc restores this aberrant phenotype have remained opaque.

Here, we demonstrate that etiolated-seedling greening is induced preferentially by Suc relative to other sugars. We further identify a Suc feedback loop. Specifically, under darkness, Suc in germinating seeds preferentially induces *ACS7* expression and associated ET biosynthesis, which in turn activates EIN3 by its canonical signal transduction pathway. Activated EIN3 directly inhibits the function of SUC2 by directly binding to the *SUC2* promoter to block Suc export from cotyledons and thereby elevate Suc accumulation in cotyledons. Therefore, under darkness, the Suc feedback loop (Suc-ACS7-ET-EIN3-|SUC2-Suc) promotes Suc accumulation by inhibiting Suc export from cotyledons to continually induce ET biosynthesis. Following white light illumination, ET-activated EIN3 directly inhibits the function of phyA to promote the cotyledon greening. Therefore, under darkness or under the mechanical stress of the soil, the feedback-loop-mediated Suc accumulation is a prerequisite for ET biosynthesis or Suc/ET signaling-mediated etiolated-seedling greening under light.

The Suc feedback loop (Suc-ACS7-ET-EIN3-|SUC2-Suc) is essential for Suc accumulation and associated ET biosynthesis

ET is a gaseous hormone that has key functions in plant growth, development, and stress responses. It has been previously reported that the mechanical stress of the soil stimulates ET production to promote etiolated-seedling greening (Zhong et al., 2014). However, the molecular mechanisms of how ET is generated under this condition have remained elusive.

Compared with other soluble exogenous sugars, Suc preferentially stimulates ET production in the leaf blades of *Arabidopsis* (Jeong et al., 2010), rice (Kobayashi and Saka, 2000), and tobacco (Philosoph-Hadas et al., 1985) in a dose-dependent manner. Further, ET production promotes etiolated-seedling greening by a key ET component, EIN3, controlling a few phytochrome and associated factors (Zhong et al., 2009). These reports suggest that Suc might induce ET production to promote etiolated-seedling greening. Further, during etiolated-seedling greening, a large amount of Suc is consumed, dependent on phytochrome (Kozuka et al., 2020). Therefore, it is probable that under darkness, Suc export from cotyledons must be blocked, or Suc must be accumulated in cotyledons to continually stimulate ET biosynthesis to promote etiolated-seedling greening, when exposed to light. However, the relative regulatory pathway is unknown.

In the present study, both *ACS7* expression (Figure 2O) and ET production (Jeong et al., 2010) were preferentially induced by the exogenous application of Suc. Further, both endogenous Suc accumulation and ET production increased gradually with age in wild-type, but not *acs7-1*, seedlings (Figures 2Q and 2R). Moreover, ET biosynthesis did not occur in *suc2-5*/+ mutant seedlings (Figure S7). These findings indicate that both ACS7 and SUC2 are essential for Suc-induced ET production. We also demonstrated that Suc/ET signaling-mediated cotyledon greening is dependent on the EIN3/EIL1 component (Figure 3). Therefore, ACS7, EIN3, and SUC2 are essential for Suc/ET signaling-mediated cotyledon greening. Further, the direct suppression of *SUC2* activity via an ACS7-EIN3 module (Figures 4 and S3) led to the suppression of Suc phloem loading in cotyledons (Figure S4), resulting in Suc accumulation in cotyledons (Figure S4). Therefore, these components form a Suc feedback loop (Suc-ACS7-ET-EIN3-|SUC2-Suc) to promote Suc accumulation in cotyledons.

Further, EIN3 is elevated, and *SUC2* transcripts were reduced under darkness (Zhong et al., 2009; Kühn et al., 1997). Darkness is known to suppresses SUC2 activity (Wright et al., 2003). These reports further suggested that Suc is constantly accumulated under subterranean darkness, probably due to the decline in the Suc-feedback-loop-mediated Suc phloem loading. Therefore, when buried seeds germinate under subterranean darkness, the accumulating Suc enables ET production by preferential inducting *ACS7* expression via the Suc feedback loop (Figure 7). Greater mechanical stress of the soil will lead to the exudation of less ET production from the soil. As a result, more ET production in the soil accelerates cotyledon greening and enables seedlings to grow out of soil.

Collectively, under darkness, these components form a Suc feedback loop (Suc-ACS7-ET-EIN3-|SUC2-Suc) to constantly promote Suc accumulation, *ACS7* expression, and associated ET biosynthesis in cotyledons, and to promote Suc/ET signaling-mediated cotyledon greening, following white light illumination (Figure 7).

The cooperation of the Suc feedback loop and the ET-EIN3-PORA/B module promotes Suc/ET signaling-mediated etiolated-seedling greening

Under darkness, Suc accumulation, *ACS7* expression, and associated ET biosynthesis in cotyledons are promoted by the Suc feedback loop (Figure 7). Following white light illumination, generated ET activates EIN3 to facilitate etiolated-seedling greening by EIN3 directly binding to the promoters of *PORA/B*, which encode key enzymes in the chlorophyll synthesis pathway

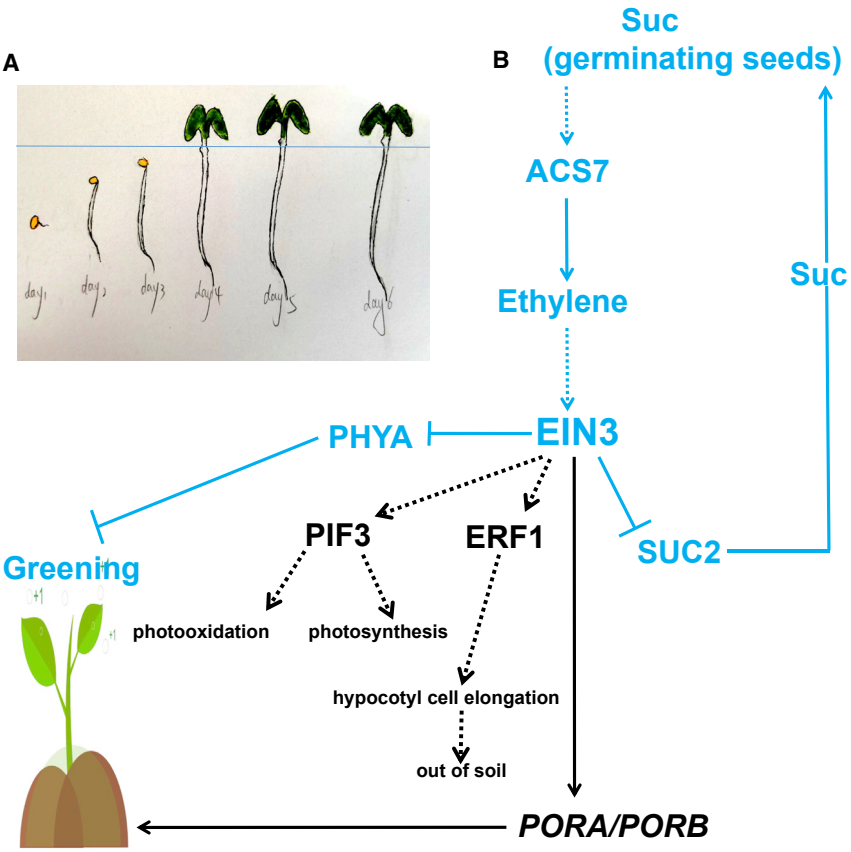

Figure 7. Model illustrating how Suc promotes cotyledon greening of etiolated seedlings by EIN3 controlling a few phytochromes and associated factors

(A) Model for cotyledon greening of etiolated seedlings.

(B) In the first step, under subterranean darkness, accumulated Suc in germinating seeds induces *ACS7* expression, related ethylene biosynthesis, and successive EIN3 activity. EIN3 subsequently directly suppresses SUC2 function, thereby inhibiting Suc phloem loading in cotyledons. Consequently, transport of cotyledon Suc into true leaves is inhibited. As a result, by virtue of a Suc-ACS7-EIN3-SUC2-Suc module, Suc accumulates in seedling cotyledons, to guarantee continual ET biosynthesis. In the second step, on seedling emergence from soil and concomitant exposure to white light irradiation, ET-activied EIN3 negatively regulates PHYA. Thus, relieving PHYA inhibition leads to etiolated-seedling greening. This canonical ethylene signal transduction pathway comprises the ethylene receptor ETR and the ethylene signaling components CTR1, EIN2, EIN3, and EIL1. Solid lines indicate direct regulation, whereas dotted lines indicate either indirect regulation or regulation in an unknown manner. Please note that in (B), blue lines represent conclusions in this study, whereas black lines represent conclusions in previous reports.

(Zhong et al., 2009). Therefore, etiolated-seedling greening is promoted by the ET-EIN3-PORA/B module. This module may be another regulatory pathway of Suc/ET signaling-mediated etiolated-seedling greening (Figure 7). Therefore, the Suc feedback loop and the ET-EIN3-PORA/B module synergistically facilitate Suc/ET signaling-mediated etiolated-seedling greening.

The Suc-ACS7-ET-EIN3-ERF1-PIF3 module promotes Suc/ET signaling-mediated etiolated seedlings and enables seedlings to grow out of soil

The EIN3/EIL1 proteins activate an ET signaling-mediated PIF3-ERF1 transcriptional circuitry to synchronously promote etiolated-seedling greening by tissue-specific patterns (Zhong et al., 2014). That is, the *EIN3/EIL1-ERF1* gene cascade modulates the cell elongation of hypocotyls. As a result, cotyledons of the etiolated seedlings are able to penetrate the soil cover. By contrast, the *EIN3/EIL1-PIF3* gene cascade synchronously regulates the preassembly of photosynthetic machinery in cotyledons (Zhong et al., 2014). The cooperation of these two processes allows etiolated seedlings to gain photosynthetic capacity but avoid being damaged through photooxidation from dark to light. However, under darkness, the Suc-feedback-loop-induced Suc accumulation is a prerequisite for ET production to activate EIN3 and thus promote sugar-ET signaling-mediated etiolated-seedling greening (Figure 7). Therefore, following white light illumination, accumulated Suc under darkness are essential for sugar-ET signaling-mediated etiolated-seedling greening by a key ET component, EIN3, controlling both *ERF1* and *PIF3* gene expression (Figure 7). Together, under subterranean darkness, ET production is promoted preferentially by Suc relative to other sugars by the Suc feedback loop to promote Suc-ET signaling-mediated etiolated-seedling greening and to enable these seedlings to grow out of the soil by the Suc-ACS7-ET-EIN3-ERF1-PIF3 module in the light (Figure 7).

Suc represents a class of regulators that function in conjunction with ET signaling, Suc transport, and a few phytochromes and EIN3 controlling a few phytochromes and associated factors to optimize the de-etiolation of *Arabidopsis* seedlings as they emerge from subterranean darkness and are exposed to light (Figure 7).

Summary of main findings in this study

In this study, we demonstrated that sugars promote etiolated-seedling greening. We identified that ACS7, CINV1/2, and SUC2 are endogenous regulators of the *Arabidopsis* etiolated-seedling greening. Further, Suc, relative to other sugars, preferentially promotes etiolated-seedling greening. We also identified a Suc feedback loop (Suc-ACS7-ET-EIN3-SUC2-Suc). This loop promotes Suc accumulation in cotyledons, and this process is essential for ET biosynthesis, EIN3 activity, and, finally, etiolated-seedling greening mediated by EIN3 controlling a few phytochromes and associated factors. Finally, we found that EIN3 inhibits phyA functions by directly binding to the *phyA* promoter to promote etiolated-seedling greening.

Limitations of the study

In this study, we have identified a Suc feedback loop (Suc-ACS7-ET-EIN3-SUC2-Suc), which is essential for ET biosynthesis, EIN3 activity, and Suc-ET signaling-mediated etiolated-seedling greening. However, the connections between Suc and ACS7 are unclear. For example, whether Suc promotes *ACS7* expression by signaling or metabolism remains unknown. Suc promotes *ACS7* expression by an unknown pathway. Moreover, cellular nitrogen and carbon metabolism are tightly coordinated to sustain optimal growth and development for plants and other cellular organisms. We currently know little about the mechanisms if cellular nitrogen regulates etiolated-seedling greening. How mineral nutrient nitrogen regulates etiolated-seedling greening remains unknown. It is also unclear whether phyA, as a key component, is involved in cellular nitrogen-mediated etiolated-seedling greening.

STAR★METHODS

Detailed methods are provided in the online version of this paper and include the following:

- KEY RESOURCES TABLE
- RESOURCE AVAILABILITY
  - Lead contact
  - Materials availability
  - Data and code availability
- EXPERIMENTAL MODEL AND SUBJECT DETAILS
- METHOD DETAILS
  - Plant materials and growth conditions
  - GUS assay and histochemical assay of GUS activity
  - Plasmid constructs
  - Quantitative PCR
  - Greening rate
  - Seedling observation and photography
  - ET assay
  - Chlorophyll content
  - Assay of sugar metabolites
  - Phloem loading of Suc
  - Histological analysis
  - Transactivation assay
  - Protein expression and purification
  - ChIP-PCR
  - Electrophoretic mobility shift assay (EMSA)
- QUANTIFICATION AND STATISTICAL ANALYSIS

SUPPLEMENTAL INFORMATION

Supplemental information can be found online at https://doi.org/10.1016/j.celrep.2022.110529.

ACKNOWLEDGMENTS

This study was supported by grants from the Priority Academic Program Development of Jiangsu Higher Education Institutions (PAPD). This work is supported by the National Natural Science Foundation of China (31770613).

AUTHOR CONTRIBUTIONS

L.-S.M. designed the experiments. L.-S.M., X.-Y.C., X.-R.M., C.T., L.-N.X., Q.-X.B., W.-Y.M., and C.-Y.L. performed the experiments. X.-Y.C, C.T., and L.-S.M. completed statistical analyses of data. L.-S.M., G.J.L., X.-T.F., and J.-H.J. wrote, edited, and revised this manuscript.

DECLARATION OF INTERESTS

The authors declare no competing interests.

Received: December 9, 2020
Revised: August 1, 2021
Accepted: February 24, 2022
Published: March 15, 2022

REFERENCES

An, F., Zhao, Q., Ji, Y., Li, W., Jiang, Z., Yu, X., Zhang, C., Han, Y., He, W., Liu, Y., et al. (2010). Ethylene-induced stabilization of ETHYLENE INSENSITIVE3 and EIN3-LIKE1 is mediated by proteasomal degradation of EIN3 binding F-box 1 and 2 that requires EIN2 in arabidopsis. Plant Cell *22*, 2384–2401.

Barnes, S.A., Nishizawa, N.K., Quaggio, R.B., Whitelam, G.C., and Chua, N.H. (1996). Far-red light blocks greening of *Arabidopsis* seedlings via a phytochrome A-mediated change in plastid development. Plant Cell *8*, 601–615.

Barnes, W.J., and Anderson, C.T. (2018). Cytosolic invertases contribute to cellulose biosynthesis and influence carbon partitioning in seedlings of *Arabidopsis thaliana*. Plant J. *94*, 956–974.

Barratt, D.H., Derbyshire, P., Findlay, K., Pike, M., Wellner, N., Lunn, J., Feil, R., Simpson, C., Maule, A.J., and Smith, A.M. (2009). Normal growth of *Arabidopsis* requires cytosolic invertase but not sucrose synthase. Proc. Natl. Acad. Sci. U S A *106*, 13124–13129.

Binder, B.M., Walker, J.M., Gagne, J.M., Emborg, T.J., Hemmann, G., Bleecker, A.B., and Vierstra, R.D. (2007). The *Arabidopsis* EIN3 binding F-Box proteins EBF1 and EBF2 have distinct but overlapping roles in ethylene signaling. Plant Cell *19*, 509–523.

Chang, K.N., Zhong, S., Weirauch, M.T., Hon, G., Pelizzola, M., Li, H., Huang, S.S., Schmitz, R.J., Urich, M.A., Kuo, D., et al. (2013). Temporal transcriptional response to ethylene gas drives growth hormone cross-regulation in *Arabidopsis*. eLife *2*, e00675.

Chen, L.Q., Qu, X.Q., Hou, B.H., Sosso, D., Osorio, S., Fernie, A.R., and Frommer, W.B. (2012). Sucrose efflux mediated by SWEET proteins as a key step for phloem transport. Science *335*, 207–211.

Chincinska, I.A., Liesche, J., Krügel, U., Michalska, J., Geigenberger, P., Grimm, B., and Kühn, C. (2008). Sucrose transporter StSUT4 from potato affects flowering, tuberization, and shade avoidance response. Plant Physiol. *146*, 515–528.

Cho, Y.H., Yoo, S.D., and Sheen, J. (2006). Regulatory functions of nuclear hexokinase1 complex in glucose signaling. Cell *127*, 579–589.

Cornah, J.E., Germain, V., Ward, J.L., Beale, M.H., and Smith, S.M. (2004). Lipid utilization, gluconeogenesis, and seedling growth in *Arabidopsis* mutants lacking the glyoxylate cycle enzyme malate synthase. J. Biol. Chem. *279*, 42916–42923.

Duek, P.D., and Fankhauser, C. (2005). bHLH class transcription factors take centre stage in phytochrome signalling. Trends Plant Sci. *10*, 51–54.

Eastmond, P.J., Germain, V., Lange, P.R., Bryce, J.H., Smith, S.M., and Graham, I.A. (2000). Postgerminative growth and lipid catabolism in oilseeds lacking the glyoxylate cycle. Proc. Natl. Acad. Sci. U S A *97*, 5669–5674.

Gottwald, J.R., Krysan, P.J., Young, J.C., Evert, R.F., and Sussman, M.R. (2000). Genetic evidence for the in planta role of phloem-specific plasma membrane sucrose transporters. Proc. Natl. Acad. Sci. U S A *97*, 13979–13984.

Graham, I.A. (2008). Seed storage oil mobilization. Annu. Rev. Plant Biol. *59*, 115–142.

Jeong, S.W., Das, P.K., Jeoung, S.C., Song, J.Y., Lee, H.K., Kim, Y.K., Kim, W.J., Park, Y.I., Yoo, S.D., Choi, S.B., et al. (2010). Ethylene suppression of sugar-induced anthocyanin pigmentation in *Arabidopsis*. Plant Physiol. *154*, 1514–1531.

Kang, C.Y., Lian, H.L., Wang, F.F., Huang, J.R., and Yang, H.Q. (2009). Cryptochromes, phytochromes, and COP1 regulate light-controlled stomatal development in *Arabidopsis*. Plant Cell *21*, 2624–2641.

Kobayashi, H., and Saka, H. (2000). Relationship between ethylene evolution and sucrose content in excised leaf blades of rice. Plant Prod. Sci. *3*, 398–403.

Kozuka, T., Sawada, Y., Imai, H., Kanai, M., Hirai, M.Y., Mano, S., Uemura, M., Nishimura, M., Kusaba, M., and Nagatani, A. (2020). Regulation of sugar and storage oil metabolism by phytochrome during de-etiolation. Plant Physiol. *182*, 1114–1129.

Kühn, C., Franceschi, V.R., Schulz, A., Lemoine, R., and Frommer, W.B. (1997). Macromolecular trafficking indicated by localization and turnover of sucrose transporters in enucleate sieve elements. Science *275*, 1298–1300.

Lei, M., Liu, Y., Zhang, B., Zhao, Y., Wang, X., Zhou, Y., Raghothama, K.G., and Liu, D. (2011). Genetic and genomic evidence that sucrose is a global regulator of plant responses to phosphate starvation in *Arabidopsis*. Plant Physiol. *156*, 1116–1130.

Leskow, C.C., Kamenetzky, L., Dominguez, P.G., Díaz Zirpolo, J.A., Obata, T., Costa, H., Martí, M., Taboga, O., Keurentjes, J., Sulpice, R., et al. (2016). Allelic differences in a vacuolar invertase affect *Arabidopsis* growth at early plant development. J. Exp. Bot. *67*, 4091–4103.

Li, Z., Peng, J.Y., Wen, X., and Guo, H. (2013). ETHYLENE-INSENSITIVE3 is a senescence-associated gene that accelerates age-dependent leaf senescence by directly repressing miR164 transcription in *Arabidopsis*. Plant Cell *25*, 3311–3328.

Lichtenthaler, H.K. (1987). Chlorophylls and carotenoids: pigments of photosynthetic biomembranes. Methods Enzymol. *18*, 350–382.

Liu, Y., and Zhang, S. (2004). Phosphorylation of 1-aminocyclopro-pane-1-carboxylic acid synthase by MPK6, a stress-responsive mitogen-activated protein kinase, induces ethylene biosynthesis in *Arabidopsis*. Plant Cell *16*, 3386–3399.

Lou, Y., Gou, J.Y., and Xue, H.W. (2007). PIP5K9, an *Arabidopsis* phosphatidylinositol monophosphate kinase, interacts with a cytosolic invertase to negatively regulate sugar-mediated root growth. Plant Cell *19*, 163–181.

Mazzella, M.A., Casal, J.J., Muschietti, J.P., and Fox, A.R. (2014). Hormonal networks involved in apical hook development in darkness and their response to light. Front. Plant Sci. *5*, 52.

Meng, L.S., Wei, Z.Q., Cao, X.Y., Tong, C., Lv, M.J., Yu, F., and Loake, G.J. (2020). Cytosolic invertase mediated root growth is feedback-regulated by A glucose-dependent signaling loop. Plant Physiol. *184*, 895–908.

Meng, L.S., and Yao, S.Q. (2015). Transcription co-activator *Arabidopsis* ANGUSTIFOLIA3 (AN3) regulates water-use efficiency and drought tolerance by modulating stomatal density and improving root architecture by the transrepression of YODA (YDA). Plant Biotechnol. J. *13*, 893–902.

Meng, L.S., Wang, Z.B., Yao, S.Q., and Liu, A. (2015). The *ARF2–ANT–COR15A* gene cascade regulates ABA signaling-mediated resistance of large seeds to drought in *Arabidopsis*. J. Cell Sci. *128*, 3922–3932.

Meng, L.S., Xu, M.K., Wan, W., Yu, F., Li, C., Wang, J.Y., Wei, Z.Q., Lv, M.J., Cao, X.Y., Li, Z.Y., et al. (2018). Sucrose signaling regulates anthocyanin biosynthesis through a MAPK cascade in *Arabidopsis thaliana*. Genetics *210*, 607–619.

Meng, L.S., Bao, Q.X., Mu, X.R., Tong, C., Cao, X.Y., Huang, J.J., Xue, L.N., Liu, C.Y., Fei, Y., and Loake, G.J. (2021). Glucose- and sucrose-signaling modules regulate the *Arabidopsis* juvenile-to-adult phase transition. Cell Rep. *36*, 109348.

Moon, J., Zhu, L., Shen, H., and Huq, E. (2008). PIF1 directly and indirectly regulates chlorophyll biosynthesis to optimize the greening process in *Arabidopsis*. Proc. Natl. Acad. Sci. U S A *105*, 9433–9438.

Philosoph-Hadas, S., Meir, S., and Aharoni, N. (1985). Carbohydrates stimulate ethylene production in tobacco leaf discs. II. Sites of stimulation in the ethylene biosynthesis pathway. Plant Physiol. *78*, 139–143.

Sergeeva, L.I., Keurentjes, J.J.B., Bentsink, L., Vonk, J., van der Plas, L.H.W., Koornneef, M., and Vreugdenhil, D. (2006). Vacuolar invertase regulates elongation of *Arabidopsis thaliana* roots as revealed by QTL and mutant analysis. Proc. Natl. Acad. Sci. U S A *103*, 2994–2999.

Sperling, U., van Cleve, B., Frick, G., Apel, K., and Armstrong, G.A. (1997). Overexpression of light-dependent PORA or PORB in plants depleted of endogenous POR by far-red light enhances seedling survival in white light and protects against photooxidative damage. Plant J. *12*, 649–658.

Srivastava, A.C., Dasgupta, K., Ajieren, E., Costilla, G., McGarry, R.C., and Ayre, B.G. (2009). *Arabidopsis* plants harbouring a mutation in AtSUC2, encoding the predominant sucrose/proton symporter necessary for efficient phloem transport, are able to complete their life cycle and produce viable seed. Ann. Bot. *104*, 1121–1128.

Srivastava, A.C., Ganesan, S., Ismail, I.O., and Ayre, B.G. (2008). Functional characterization of the *Arabidopsis* AtSUC2 sucrose/H 1 symporter by tissue-specific complementation reveals an essential role in phloem loading but not in long-distance transport. Plant Physiol. *148*, 200–211.

Stadler, R., and Sauer, N. (1996). The *Arabidopsis thaliana AtSUC2* gene is specifically expressed in companion cells. Bot. Acta *109*, 299–306.

Stadler, R., Brandner, j., Schulz, A., Gahrtz, M., and Sauer, N. (1995). Phloem loading by the PmSUC2 sucrose carrier from Plantago major occurs into companion cells. Plant Cell *7*, 1545–1554.

Stephenson, P.G., Fankhauser, C., and Terry, M.J. (2009). PIF3 is a repressor of chloroplast development. Proc. Natl. Acad. Sci. U S A *106*, 7654–7659.

Sun, X.D., Feng, Z.H., and Meng, L.S. (2012). Ectopic expression of the *Arabidopsis* ASYMMETRIC LEAVES2-LIKE5 (ASL5) gene in cockscomb (*Celosia cristata*) generates vascular-pattern modifications in lateral organs. Plant Cell Tiss. Organ Cult. *110*, 163–169.

Wright, K.M., Roberts, A.G., Martens, H.J., Sauer, N., and Oparka, K.J. (2003). Structural and functional vein maturation in developing tobacco leaves in relation to AtSUC2 promoter activity. Plant Physiol. *131*, 1555–1565.

Xu, C., Hao, B., Sun, G., Mei, Y., Sun, L., Sun, Y., Wang, Y., Zhang, Y., Zhang, W., Zhang, M., et al. (2021). Dual activities of ACC synthase: novel clues regarding the molecular evolution of ACS genes. Sci. Adv. *7*, eabg8752. https://doi.org/10.1126/sciadv.abg8752.

Xu, Q., Chen, S., Yunjuan, R., Chen, S., and Liesche, J. (2018). Regulation of sucrose transporters and phloem loading in response to environmental cues. Plant Physiol. *176*, 930–945.

Yanagisawa, S., Yoo, S.D., and Sheen, J. (2003). Differential regulation of EIN3 stability by glucose and ethylene signaling in plants. Nature *425*, 521–525.

Yang, S., Wang, S., Li, S., Du, Q., Qi, L., Wang, W., Chen, J., and Wang, H. (2020). Activation of ACS7 in *Arabidopsis* affects vascular development and demonstrates a link between ethylene synthesis and cambial activity. J. Exp. Bot. https://doi.org/10.1093/jxb/eraa423.

Yoo, S.D., Cho, Y.H., Tena, G., Xiong, Y., and Sheen, J. (2008). Dual control of nuclear EIN3 by bifurcate MAPK cascades in C2H4 signalling. Nature *451*, 789–795.

Zhong, S., Shi, H., Xue, C., Wei, N., Guo, H., and Deng, X.W. (2014). Ethylene-orchestrated circuitry coordinates a seedlings response to soil cover and etiolated growth. Proc. Natl. Acad. Sci. U S A *111*, 3913–3920.

Zhong, S., Zhao, M., Shi, T., Shi, H., An, F., Zhao, Q., and Guo, H. (2009). EIN3/EIL1 cooperate with PIF1 to prevent photo-oxidation and to promote greening of *Arabidopsis* seedlings. Proc. Natl. Acad. Sci. U S A *106*, 21431–21436.

STAR★METHODS

KEY RESOURCES TABLE

REAGENT or RESOURCE	SOURCE	IDENTIFIER
Critical commercial assays		
GUS staining Kit	COOLABER SCIENCE & TECHNOLOGY Co.,LTD	Cat#SL7160
TRIZOL reagent	Invitrogen, Carlsbad, CA, USA	N/A
Plant Suc assay kit	Beijing Solarbio Science & Technology Co., Ltd, http://www.solarbio.com/goods-9298.html	Cat#BC2465
LightShift Chemiluminescent EMSA Kit	Beyotime Biotechnology, http://www.beyotime.com	Cat#GS009
Experimental models: Organisms/strains		
E. coli (Rosetta2)	N/A	N/A
*Arabidopsis:*WT Col-0	N/A	N/A
*Arabidopsis:*5 × *EBS-GUS* /wild-type	Li et al., 2013	N/A
Arabidopsis:phyA(CS6223)	Kang et al., 2009	N/A
Arabidopsis:ein3-1	An et al., 2010	N/A
Arabidopsis:ein3/eil1	An et al., 2010	N/A
Arabidopsis:35S:SUC2	Lei et al., 2011	N/A
Arabidopsis:suc2-5	Lei et al., 2011	N/A
Arabidopsis:FLAG-EIN3	An et al., 2010	N/A
Arabidopsis:35S:EIN3-GFP	An et al., 2010	N/A
Arabidopsis:acs2(SALK_208272C)	AraShare,http://www.arashare.cn	N/A
Arabidopsis:acs4(SALK_068371C)	AraShare,http://www.arashare.cn	N/A
Arabidopsis:acs6(SALK_138142C)	AraShare,http://www.arashare.cn	N/A
Arabidopsis:acs7-1(CS16570)	Prof N.N Wang (NanKai University, China)	N/A
Oligonucleotides		
Primers used in this study	This study; Table S1	N/A
Recombinant DNA		
pHB:EIN3-GFP/SUC2(mEBS)pro::SUC2	This study	N/A
pHB:EIN3-GFP/phyA(mEBS)pro::phyA	This study	N/A
pCB308R:ACS7-GUS	This study	N/A
EIN3pro::EIN3-GFP	This study	N/A
pCB2004:ACS7	This study	N/A
proSUC2-LUC	This study	N/A
MproSUC2-LUC	This study	N/A
pGreen-mSUC2	This study	N/A
pGreen-mphyA	This study	N/A
pGreen-mSUC2/EIN3	This study	N/A
pGreen-mphyA/EIN3	This study	N/A
Software and algorithms		
Image J	Image J	https://imagej.nih.gov/ij/
Graph Pad Prism	Graph Pad Software	https://www.graphpad.com/

RESOURCE AVAILABILITY

Lead contact

Further information and requests for resources and reagents should be directed to and will be fulfilled by the lead contact, Lai-Sheng Meng (menglsh@jsnu.edu.cn).

Materials availability

All unique/stable reagents generated in this study are available from the lead contact without restriction.

Data and code availability

This paper does not report original code. ''Any additional information required to reanalyze the data reported in this paper is available from the lead contact upon request.''

EXPERIMENTAL MODEL AND SUBJECT DETAILS

All plants are in the Col-0 background, unless indicated differently. Seedlings grown on agar were maintained in a growth room under a 16/8 h of light/dark cycle with cool white fluorescent light at 21 ± 2°C. Plants grown in soil were maintained in a controlled environmental growth chamber under a 16/8 h light/dark cycle with white light [60 (low light), 130 (middle light/normal), 230 (high light) μmol quanta PAR m^{-2} s^{-1}] conditions at 21 ± 2°C. Unless otherwise stated, seedlings grown on agar were under middle light conditions at 21 ± 2°C.

METHOD DETAILS

Plant materials and growth conditions

The *5 × EBS-GUS*/wild-type (Li et al., 2013), *phyA* (CS6223) (Kang et al., 2009), *ein3-1* and *ein3/eil1* (An et al., 2010) mutants, *35S:SUC2* and *suc2-5* (Lei et al., 2011), *5 × EBS-GUS* (Li et al., 2013), *FLAG-EIN3* and *35S:EIN3-GFP* (An et al., 2010) were all described previously.

The *35S:EIN3-GFP*, *ein3/eil,* and *ein3-1* seeds were kindly provided by Prof H. W. Guo (South University of Science and Technology of China, China). *pGreen0800-LUC* vector and *5×EBS:GUS* seeds were kindly provided by Associate Prof Ziqiang Zhu (Nanjing Normal University, Nanjing, China). The *35S:SUC2* and *suc2-5* (SALK_087046) seeds were kindly provided by Prof D Liu (Tsinghua University, China). The *phyA* (CS6223) mutant were obtained from the ABRC (Ohio State University). The *acs2* (SALK_208272C), *acs4* (SALK_068371C), *acs6* (SALK_138142C) mutants were requested from AraShare (a non-profit *Arabidopsis* share center, http://www.arashare.cn).The *acs7-1* (CS16570) seeds were kindly provided by Prof N.N Wang (NanKai University, China).

The *ein3/eil1/phyA* mutant was obtained from F2 plants [*ein3/eil1/phyA* (CS6223)] that have long hypocotyl and unexpanded cotyledons in far-red light (Barnes et al., 1996) and have elongated hypocotyls on solid MS medium with 6.0 μm ACC (An et al., 2010). The *ein3/eil1/suc2*/+ mutant was obtained from F2 plants (*ein3/eil1/suc2-5*/+) that had elongated hypocotyls on solid MS medium with 6.0 μm ACC (An et al., 2010) and then were identified through PCR-based genotyping for *suc2-5*/+.

For simultaneous germination, seeds were treated with jarovization at 4°C overnight and then sown on solid MS medium supplemented with 1% Suc, pH 5.8 and 0.8% agar (Meng and Yao., 2015). Seedlings grown on agar were maintained in a growth room under a 16/8 h of light/dark cycle with cool white fluorescent light at 21 ± 2°C (5). Plants grown in soil were maintained in a controlled environmental growth chamber under a 16/8 h light/dark cycle with white light [60 (low light), 130 (middle light/normal), 230 (high light) μmol quanta PAR m^{-2} s^{-1}] conditions at 21 ± 2°C. Unless otherwise stated, seedlings grown on agar were under middle light conditions at 21 ± 2°C.

Wild-type is Col-0 unless otherwise stated. In all experiments, three biological replicates were performed and error bars represent SD.

GUS assay and histochemical assay of GUS activity

Using a mix buffer (1 mM X-gluc, 60 mM NaPO4 buffer, 0.4 mM of K3Fe(CN)6/K4Fe(CN)6 and 0.1% (v/v) Triton X-100), samples (Transgenic plants harboring and expressing *5×EBS (EIN3 binding site)-GUS, ACS7pro-GUS*) were stained, and then incubated at 37°C for 8 h. After GUS staining, In each process, 30,50,70,90,90,100% ethanol was used to remove the chlorophyll for about 30 min.

Plasmid constructs

For obtaining *pHB:EIN3-GFP/SUC2(mEBS)pro::SUC2* plasmid, (1) Used primers were SUC2pcpF; R-M-EMSA-SUC2 and M-EMSA-SUC2; SUC2pcR for gaining *SUC2* promoter sequence. (2) Used primers were SUC2pcF; SUC2pcpR for gaining *SUC2* CDS sequence. (3) Using *PHB-35S-3×FLAG-EIN3* plasmid as template, used primers were 35SEIN3TERF; 35SEIN3TERR for gaining *35S-3×FLAG-EIN-ter*. (4) using EcoRI and XbaI, *35S-3×FLAG-EIN-ter* plasmid was digested. (5) Using ClonExpress II One Step Cloning Kit, above four fragments were linked to *pHB:EIN3-GFP/SUC2(mEBS)pro::SUC2* plasmid. Using the same method, we generated *pHB:EIN3-GFP/phyA(mEBS)pro::phyA* plasmid. In detail, (1) used primers were phyApcpF; R-M-EMSA-phyA and M-EMSA-phyA; phyApcR for generating the *phyA* promoter sequence. (2) Used primers were phyApcF; phyApcpR for gaining *phyA* CDS sequence. (3) Using *PHB-35S-3×FLAG-EIN3* plasmid as template, used primers were 35SEIN3TERF; 35SEIN3TERR for gaining *35S-3×FLAG-EIN-ter*. (4) Using EcoRI and XbaI, *35S-3×FLAG-EIN-ter* plasmid was digested. (5) Using ClonExpress II One Step Cloning Kit, above four fragments were linked to *pHB:EIN3-GFP/phyA(mEBS)pro::phyA* plasmid.

For obtaining *pCB308R:ACS7-GUS* plasmid, used primers can be seen in Table S1.

For obtaining *EIN3pro::EIN3-GFP* plasmid, used primers can be seen in Table S1.

For obtaining *pCB2004:ACS7* plasmid, used primers can be seen in Table S1.

Quantitative PCR

Total RNA was prepared from tissues indicated in the figures by the TRIZOL reagent (Invitrogen), and 1 μg of RNA from each sample was used for the reverse transcription reaction. Subsequently, 1 μL of the reverse transcription reaction was used as template for PCR amplification. The same RNA samples and primers were used for real-time PCR analysis that was performed and statistically analyzed as described (Meng et al., 2021). Kinetic detection of PCR products using Sybrgreen real-time RT-PCR. As an internal control, Tubulin transcripts were used to quantify the relative transcriptional level of each target gene in each tissue type. Primer pairs are listed in Table S2. Unless otherwise specified, the number of PCR cycles is 30. Three repeated biological experiments were carried out.Primer pairs of *SUC2* were utilized. Primer pairs of *EIN3* have been described by (Meng et al., 2018). Primer pairs of *ACS7* were utilized. Used primers can be seen in Table S1.

Greening rate

For determining the greening rate, ≥ 40 seedlings were grown on solid MS medium with the indicated sugar concentration under darkness for the indicated number of days after germination and then transferred into white light ([60 (low light), 130 (middle light), 230 (high light) μmol quanta PAR m^{-2} s^{-1}] to grow for the given time. The greening rate was calculated as the percentage of seedlings exhibiting greening, as described (Zhong et al., 2009).

Seedling observation and photography

Different age seedlings were observed and photographed by using stereo microscope [Leica Microsystems (Switzerland) Ltd. CH-9435 Heerbrugg. Type: DMC4500 (12730517)].

ET assay

Experiments performed on indicated-day-old seedlings using a gas chromatograph equipped with a flame ionization detector [Echrom Technologies (shanghai) Ltd Co], For ethylene collection, petri dishes containing indicated-day-old seedlings were opened to remove trapped air, and then the original lids were replaced by lids with silicone rubber seals. After a further 24 h of incubation under the same conditions, 1 mL of gas was withdrawn from each plate using a gas-tight syringe. The gas was injected into a gas chromatograph equipped with a flame ionization detector [Echrom Technologies (shanghai) Ltd Co]. The carrier gas (N2) flow rate was 60 mL min−1. The detector response was standardized by injecting known amounts of ethylene prepared by serial dilution. Means and sd values were calculated from three experiments.

Chlorophyll content

Chlorophyll content was extracted from cotyledons of five or six-day-old etiolated seedlings followed by 1 day of white light irradiation through boiling them in 95% ethanol at 80°C. The chlorophyll concentration per fresh weight of cotyledons of the same weight was examined, as has been described by Lichtenthaler (1987).

Assay of sugar metabolites

Plant Suc assay kit (Beijing Solarbio Science & Technology Co., Ltd, Cat#BC2465; http://www.solarbio.com/goods-9298.html) was used for assay of sugar metabolites. 0.1g mature leaf blades were ground into homogenate at 23°C and 0.5 mL extraction buffer added and ground within centrifuge tube, finally kept at 80°C for 10 min and shaken 3–5 times. After cooling these extracts were centrifuged at 4,000g for 10 min, the supernatant was transferred to a fresh tube and 2 mg reagent 5 added to decolorize at 80°C for 30 min. Then 0.5 mL extraction buffer was added, mixed and centrifuged at 4,000g for 10 min. The supernatant was transferred to a fresh tube for visible light analysis.

Three centrifuged tubes per sample were used each with 25 μL of sample and then standard product (reagent 1) and water were added, respectively. Fifteen μL of reagent 2 was added, mixed and boiled at 100°C for 5 min. Subsequently, 175μL of reagent 3 and 50μL of reagent 4 were added, respectively. The resulting solution was boiled in water for 10 min, followed by measurement of the light absorption value at 480 nm after cooling. The Suc content was calculated for each sample.

Phloem loading of Suc

Nine-day-old seedlings grown on solid MS medium with or without sugars were used to assay phloem loading of Suc. Following incubation in pretreatment solution (pH5.7; liquid MS medium) for 40–50 min, the cotyledons were incubated in the phloem loading buffer (pH 5.7; MS medium with 0.1–0.2% Suc) with [^{14} C] Suc (0.50μCi mL^{-1}) and then were cultivated for 2–3 h. Following three washes in desorption solution (pH 5.7; liquid MS medium and 1% Suc), these seedlings were placed in scintillation vials and 3.0 mL of scintillation cocktail was added. The amount of [^{14} C] phloem Suc loading was analyzed using a scintillation counter and expressed as cpm mg^{-1} fresh weight.

Histological analysis

Histological analysis was performed, as was described by Sun et al. (2012). In details, leaf and cotyledon tissues were fixed in FAA (acetic acid 5% and formaldehyde 3.7% in 50% ethanol) for over 2 h, at 4°C. These tissues were dehydrated for 45–60 min in 30, 50, 70, 85, 93, 100% ethanol, followed by 2:1, 1:1, 1:2 ethanol/xylol (v/v), and 100% xylol solutions, followed by infiltration with Paraffin

(Leica, Germany) at 65°C. And then these materials were embedded in Paraffin. The sections were made by using a Microtome (Leica, Germany), and then stained with Fast Green FCF and Safranine O. These materials were placed on glass slides, and visualized by using an optical microscope (Olympus 80i, Olympus Corporation, Japan).

Transactivation assay

To examine if EIN3 activates *SUC2* expression by LUC activity assay, we performed the below experiments. To generate *proSUC2-LUC*, the promoter was PCR amplified with primers *proSUC2-F* and *proSUC2-R* from the gnomic DNA of *Arabidopsis* and inserted into the cloning site of the *pGreen0800-LUC* vector.

The *MproSUC2-LUC* construct containing mutations in the S2 sequence of the *SUC2* promoter was generated using overlap extension PCR with primers and inserted into *pGreen0800-LUC* vector. Two fragments of *MproSUC2* were combined into a integrated fragments of *MproSUC2* by using primers. Similarly, two fragments of *Mpro-phyA* were combined into an integrated fragment of *Mpro-phyA* by using primers. The primers used can be seen in Table S1.

Agrobacteria with the effector or reporter constructs were coincubated for 3 h and then infiltrated into 20-day-old *N. Benthamiana* leaf blades. Leaf blades of these seedlings were incubated under light conditions (130 μmol quanta PAR m^{-2} s^{-1}) for 2–4 days after infiltration. The firefly LUC activities were photographed after spraying with 1 mM luciferin. To determine the dual luciferase activities, firefly luciferase and *Renilla* luciferase were measured, as has been previously described (Li et al., 2013).

Protein expression and purification

The plasmid *pGEX-5X-1* for *EIN3* was utilized. The coding sequence of *EIN3* was amplified by the primer pair and cloned into the BamH1 and XhoI restriction sites of *pGEX-5X-1*. Recombinant glutathione S-transferase binding protein (GST)-tagged EIN3 was extracted from transformed *E. coli* (*Rosetta2*) after 10 h of incubation at 16°C following induction with 10 μM isopropylβ-D-1-thiogalactopyranoside. These recombinant proteins were purified using GST-agarose affinity. The primers used can be seen in Table S1.

ChIP-PCR

The transgenic lines containing *EIN3pro::EIN3-GFP* were utilized. ChIP was performed with seedlings (Meng et al., 2015, 2018). Leaf blades were incubated in buffer (1.0 mM PMSF, 0.5 M Suc, 1mM EDTA, 10–12 mM Tris, pH8.0, and 1% formaldehyde) under vacuum for 15–20 min for crosslinking the chromatin. Then, 0.1 M Gly was placed in the mixture, incubating for an additional 5 min for terminating the reaction. Leaf blades were placed and ground in liquid nitrogen and re-suspended in lysis buffer (150mM NaCl,1mM EDTA, 0.1% SDS, 0.1% deoxycholate, 50 mM HEPES, pH7.5, 1% Triton X-100, 10 mM Na-butyrate, 1 mM PMSF and 13 complete protease inhibitor (Roche). Chromatin was sheared to about 200–500 bp fragments via sonication followed by centrifuged. At 4°C, supernatants were precleared under protein G agarose beads for 1-1.5 h. Input material (supernatant containing chromatin) was used for immunoprecipitation with anti-GFP antibody. Anti-GFP antibody bound to EIN3-FLAG or GFP-chromatin complexes was incubated with protein G agarose beads for 1–1.5 h at 4–6°C and then washed several times and eluted with elution buffer. Input and immunoprecipitated chromatin were uncross-linked for 6 h at 6°C with 5M NaCl. Immunoprecipitated chromatin and input were used for PCR analysis The ChIP DNA products were analyzed PCR using two pairs of primers that were synthesized to amplify ~200 bp DNA fragments in the promoter region of *SUC2*. Primer sequences were also used for *phyA*. All used primers can be seen in Table S1.

Electrophoretic mobility shift assay (EMSA)

According to the manufacturer's instructions, the LightShift chemiluminescence EMSA kit (Beyotime Biotechnology,cat#gs009; http://www.beyotime.com) was used to detect the electrophoretic mobility shift assay (EMSA). The biotin-labeled SUC2 DNA fragments (5'-caccatttatgtttatattttcaaattatttaatacatttcaatatttcataagtgt-3' ;5'-acacttatgaaatattgaaatgtattaaataatttgaaaatataaacataaatggtg-3') and mutated SUC2 DNA fragments (5'-caccatttatgtttatattttGGGattatttaatGcGtttcaatatttcataagtgt-3' ;5'-acacttatgaaatattgaaaCgCattaaataatCCCaaaatataaacataaatggtg-3') were synthesized. The biotin-labeled phyA DNA fragments (5'-cctTTTGAAaggtatagctagctataaagactcttaagagtttattattgagtctactttatgtatgtagctgtgTTTGAAtcttg-3' ;5'-caagaTTCAAAcacagctacatacataaagtagactcaataataaactcttaagagtctttatagctagctatacctTTCAAAagg-3') and mutated phyA DNA fragments (5'-cctAAAGAAaggtatagctagctataaagactcttaagagtttattattgagtctactttatgtatgtagctgtgAAAGAAtcttg-3' ;5'-caagaTTCTTTcacagctacatacataaagtagactcaataataaactcttaagagtctttatagctagctatacctTTCTTTagg-3') were synthesized. They were annealed and used as probes, and the biotin-unlabeled same DNA fragments as competitors in this assay. The probes were incubated with the EIN3 fusion protein at room temperature for 10 min in EMSA/gel shift binding buffer (5x) (beyotime biotechnology, cat#gs005; http://www.beyotime.com). In addition to the proportional increase in the use of mutant and free probes, Each 10 μL binding reaction contains biotin-labeled probe and 5 mg protein were incubated at room temperature for 30 min. And then, we analyzed the reaction products by using 6.0% native polyacrylamide gel electrophoresis. Preparation 10 × TBE buffer (containing 891.5 mM Tris; 890 mM boric acid; and 25.5 mM EDTA, pH 8.3) for further use. Dilute 10 × TBE buffer into 0.5 × TBE buffer, Electrophoresis was performed at 60 V for about 1–2 h in 0.5 × TBE buffer at 4°C. The DNA fragments on the gel were transferred onto a nitrocellulose membrane with 0.5× TBE at 380mA for 90 min. The DNA was cross-linked onto the membrane, and the membrane was incubated in the blocking buffer for 15 min with gentle shaking; the membrane was then transferred into a blocking buffer for 15 min with gentle shaking, which comprised 5 μL of Streptavidin-HRP Conjugate with 10 mL of blocking buffer, according to the manufacturer's protocol. Dilute 10 × Wash buffer to 1× Wash buffer,

the membrane was washed 1 min with 1× washing buffer, and then washed 4 times for 5 min each with 1× washing buffer, and then the membrane was transferred into the detection of equilibrium liquid for 5 min with gentle shaking. The biotin-labeled DNA was detected by chemiluminescence according to the manufacturer's protocol.

QUANTIFICATION AND STATISTICAL ANALYSIS

Student's *t* test was used to determine the statistical significance between wild-type and mutant lines in measure related to glucose and sucrose levels, invertase activity, qPCR, chlorophyll concentration, luminescence intensity (*$p < 0.05$; **$p < 0.01$; ***$p < 0.001$).